Susceptibility of Chimeric Mice with Livers Repopulated by Serially Subcultured Human Hepatocytes to Hepatitis B Virus

Rie Utoh,[1] Chise Tateno,[1,2] Chihiro Yamasaki,[1] Nobuhiko Hiraga,[3] Miho Kataoka,[1] Takashi Shimada,[4] Kazuaki Chayama,[2,3] and Katsutoshi Yoshizato[1,2,5]

We previously identified a small population of replicative hepatocytes in long-term cultures of human adult parenchymal hepatocytes (PHs) at a frequency of 0.01%-0.09%. These hepatocytes were able to grow continuously through serial subcultures as colony-forming parenchymal hepatocytes (CFPHs). In the present study, we generated gene expression profiles for cultured CFPHs and found that they expressed cytokeratin 19, CD90 (Thy-1), and CD44, but not mature hepatocyte markers such as tryptophan-2,3-dioxygenase (TO) and glucose-6-phosphatase (G6P), confirming that these cells are hepatic progenitor-like cells. The cultured CFPHs were resistant to infection with human hepatitis B virus (HBV). To examine the growth and differentiation capacity of the cells *in vivo*, serially subcultured CFPHs were transplanted into the progeny of a cross between albumin promoter/enhancer-driven urokinase plasminogen activator-transgenic mice and severe combined immunodeficient (SCID) mice. The cells were engrafted into the liver and were able to grow for at least 10 weeks, ultimately reaching a maximum occupancy rate of 27%. The CFPHs in the host liver expressed differentiation markers such as TO, G6P, and cytochrome P450 subtypes and could be infected with HBV. CFPH-chimeric mice with a relatively high replacement rate exhibited viremia and had high serum levels of hepatitis B surface antigen. *Conclusion:* Serially subcultured human hepatic progenitor-like cells from postnatal livers successfully repopulated injured livers and exhibited several phenotypes of mature hepatocytes, including susceptibility to HBV. *In vitro*–expanded CFPHs can be used to characterize the differentiation state of human hepatic progenitor-like cells. (HEPATOLOGY 2008;47:000-000.)

Abbreviations: 9MM, 9-month-old Caucasian male; 10YF, 10-year-old Caucasian female; 12YM, 12-year-old Asian male; 16YF, 16-year-old Asian female; AAT, α1-antitrypsin; AFP, α-fetoprotein; ALB, albumin; BGP, biliary glycoprotein; BrdU, 5-bromo-2'-deoxyuridine; CFPH, colony-forming parenchymal hepatocyte; CK, cytokeratin; G6P, glucose-6-phosphatase; h, human; HBsAg, hepatitis B surface antigen; HBV, hepatitis B virus; CYP, cytochrome P450; m, mouse; MDR, multidrug resistance protein; MRP, multidrug resistance-associated protein; PH, parenchymal hepatocyte; RI, replacement index; RT-PCR, reverse-transcription polymerase chain reaction; SH, small hepatocyte; TO, tryptophan-2,3-dioxygenase; uPA, urokinase plasminogen activator.

From the [1]Yoshizato Project, Cooperative Link of Unique Science and Technology for Economy Revitalization (CLUSTER), Hiroshima Prefectural Institute of Industrial Science and Technology, Hiroshima, Japan; the [2]Hiroshima University Liver Project Research Center, Hiroshima, Japan; the [3]Division of Frontier Medical Science, Department of Medicine and Molecular Science, Programs for Biomedical Research, Graduate School of Biomedical Sciences, Hiroshima University, Hiroshima, Japan; [4]PhoenixBio Co., Ltd., Hiroshima, Japan; and the [5]Developmental Biology Laboratory and Hiroshima University 21st Century COE Program for Advanced Radiation Casualty Medicine, Department of Biological Science, Graduate School of Science, Hiroshima University, Hiroshima, Japan.

Received March 20, 2007; accepted September 18, 2007.

Supported by the Cooperative Link of Unique Science and Technology for Economy Revitalization (CLUSTER); Promotion of Science and Technology in Regional Areas; Ministry of Education, Culture, Sports, Science and Technology, Japan.

Present address for Rie Utoh: Institute of Advanced Biomedical Engineering and Science, Tokyo Women's Medical University, Tokyo, Japan.

Present address for Chise Tateno, Chihiro Yamasaki, and Katsutoshi Yoshizato: PhoenixBio Co., Ltd., Hiroshima, Japan.

Address reprint requests to: Katsutoshi Yoshizato, Ph.D., PhoenixBio Co., Ltd., 3-4-1 Kagamiyama, Higashihiroshima, Hiroshima 739-0046, Japan. E-mail: katsutoshi.yoshizato@phoenixbio.co.jp; fax: (81)-82-431-0017.

Published online in Wiley InterScience (www.interscience.wiley.com).

DOI 10.1002/hep.22057

Potential conflict of interest: Nothing to report.

Studies using rodents with damaged livers have shown that parenchymal hepatocytes (PHs) have great growth potential. When mouse (*m*) hepatocytes were transplanted into the livers of albumin promoter/enhancer-driven urokinase plasminogen activator (uPA)-transgenic mice,[1] they engrafted and repopulated the host liver. Serial transplantation experiments using *m*-hepatocytes in mice with tyrosinemia showed their enormous growth capacity.[2] The replicative potential of rat hepatocytes has also been demonstrated by transplanting them into the partially hepatectomized liver of a retrorsine-treated rat,[3] and uPA-transgenic mice crossed with severely immunodeficient mice, such as severe combined immunodeficient (SCID)/beige mice,[4] SCID mice,[5,6] or recombination activation gene 2 knockout mice[7] have been used to show the growth potential of human (*h*)-hepatocytes. When transplanted into uPA/SCID mice, PHs from a human juvenile male grew in the host liver to a level at which the proportion (replacement index) of the area of repopulated *h*-hepatocytes to the total number (host and donor) of hepatocytes reached 96% at 64 days posttransplantation.[5] Such *h*-hepatocyte–chimeric mice have been used to study the pharmacological responses of *h*-hepatocytes[5] and to investigate *h*-hepatitis viral infections.[4,6-8]

In contrast, normal hepatocytes have limited replicative capacity *in vitro* and acquire an abnormal phenotype if they are cultured for extended periods.[9,10] Studies on hepatocytes cultured in a newly devised medium (hepatocyte clonal growth medium[11,12]) revealed a subpopulation of highly replicative PHs, known as small hepatocytes (SHs), in both rats[12] and humans.[13] Their occupancy rate in *h*-liver ranged from 0.01% to 0.09% and was dependent on donor age.[13] The *h*-SHs formed colonies and grew continuously through several subcultures, which led us to name them colony-forming PHs (CFPHs).[13] Replication of the CFPHs was donor age–dependent up to passage 7 ($p = 7$),[13] and the cells did not exhibit a normal hepatocytic phenotype. Instead, they exhibited the traits of hepatocytes or biliary cells depending on the culture conditions. In addition, the CFPHs were not susceptible to infection with hepatitis B virus (HBV) (unpublished data).

In this study, we generated gene expression profiles of CFPHs and transplanted serially subcultured CFPHs into homozygous uPA/SCID mice to examine their growth and differentiation capacity. Our results indicate that the cells were engrafted onto the liver parenchyma and repopulated the tissue, ultimately differentiating into mature hepatocytes. Importantly, the *in vitro*–propagated CFPHs became susceptible to infection with HBV. This study supports our previous suggestion that CFPHs from *h*-postnatal liver are hepatic progenitor-like cells with the potential to assume a normal hepatocytic phenotype.[13]

Materials and Methods

h-*Hepatocytes.* This study was performed with the approval of the Hiroshima Prefectural Institute of Industrial Science and Technology Ethics Board. PHs were isolated as described[13,14] from livers donated by a 12-year-old Asian male (12YM) and a 16-year-old Asian female (16YF) according to the guidelines of the 1975 Declaration of Helsinki. Cryopreserved PHs from a 9-month-old Caucasian male (9MM) and a 10-year-old Caucasian female (10YF) were obtained from In Vitro Technologies (Baltimore, MD) and BD Biosciences (San Jose, CA), respectively.

Culture of CFPHs. Cryopreserved PHs from the 9MM, 12YM, and 16YF were thawed[5] and serially subcultured to obtain *in vitro*–expanded CFPHs.[13] Commercial 9MM PHs and freshly isolated 12YM and 16YF PHs were each subcultured to $p = 3$. The expanded cells were then cryopreserved, thawed upon use, and cultured on collagen-coated plates for 14-20 days as described.[13]

Flow Cytometry. We detached 12YM CFPHs ($p = 4$ or 5) from culture plates by treatment with 0.25% Trypsin-EDTA (Invitrogen, Carlsbad, CA), suspended, incubated on ice for 30 minutes with *m*-monoclonal antibodies against *h*Thy-1 (clone F15-42-1; Chemicon, Temecula, CA), and incubated with antibodies against *m*-immunoglobulin G Alexa-488 (Molecular Probes, Eugene, OR). We used *m*-immunoglobulin G_1 as a negative control. The cells were then analyzed and separated using a fluorescence-activated cell sorter (Becton Dickinson, Franklin Lakes, NJ) as reported.[12]

Transplantation of PHs and CFPHs. We detached 9MM and 12YM CFPHs ($p = 4$) from their culture plates and treated for 1 hour with DMEM containing 10% fetal bovine serum and 3 μg/mL anti–*h*-integrin α1 monoclonal antibodies (clone FB12, Chemicon).[15] This procedure improved engraftment of the CFPHs in uPA/SCID *m*-liver and reduced host mortality.

Transplantation of PHs and CFPHs was performed as described previously.[5] Homozygous uPA/SCID mice were injected with 0.75×10^6 9MM and 12YM PHs or $0.75\text{-}1.0 \times 10^6$ *in vitro*–expanded 9MM and 12YM CFPHs into the inferior splenic pole. When necessary, 10 mM 5-bromo-2′-deoxyuridine (BrdU) (Sigma, St. Louis, MO) and 1.2 mM 5-fluoro-2′-deoxyuridine (Wako, Osaka, Japan) in saline were injected intraperitoneally into the mice at 10 μL/g body weight 1 hour prior to death. The animals were treated according to the guidelines of our local committee on animal experiments.

Table 1. Summary of CFPH and PH Transplantation Experiments in uPA/SCID Mice

Group	Donor Cells	Time of Sacrifice (Weeks After Transplantation)	No. of Transplanted Mice	No. of Mice with Engraftment* [RE (%)]	RI† [Mean ± SD (n)]
A	12YM CFPHs (p = 4)	3	9	3 (33)	0.06-0.19% [0.14 ± 0.07% (n = 3)]
B	9MM CFPHs (p = 4)	3	6	4 (67)	0.03-0.05% [0.04 ± 0.01% (n = 4)]
C	9MM PHs	3	3	3 (100)	5.1-19.4% [6.4 ± 2.9% (n = 3)]
D	12YM CFPHs (p = 4)	9-10	27	14 (52)	0.2-27.0% [6.6 ± 8.3% (n = 14)]
E	9MM PHs	10-11	23‡	23 (100)‡	32.6-82.2% [57.4% (n = 2)]
F	12YM PHs	10	6	4 (67)	31.0-77.0% [62.3 ± 23.8% (n = 4)]
G§	12YM CFPHs (p = 4)	17-20	4	ND	ND

Abbreviation: ND, not determined.

*Number of mice whose livers were engrafted with transplanted PHs or CFPHs. The RE was determined via *h*ALB immunohistochemistry on sections prepared from 5 lobes of a liver.

†Ranges of RI of chimeric mice used in each group.

‡Data from Tateno et al.[5]

§Mice from group G were used for HBV infection studies.

We transplanted 9MM and 12YM CFPHs into 6 and 40 uPA/SCID mice, respectively. The mice were then killed 3, 9, or 10 weeks later, depending on the experimental purpose. In a previous report, we used 9MM and 12YM PHs as donor cells.[5] In this study, we used some of the preserved livers from these mice for histological examinations and as sources of RNA for reverse-transcription polymerase chain reaction (RT-PCR) analysis. The mice used in our transplantation experiments were separated into 7 groups (A-G) as shown in Table 1, which includes the rates of engraftment and replacement indices (RIs) of the chimeric mice.

Blood samples (5 μL) were collected periodically after transplantation from the tail veins of the hosts, and the level of *h*-albumin (ALB) in each was determined using a Human Albumin ELISA Quantitation Kit (Bethyl Laboratories, Montgomery, TX) to monitor the growth of the transplanted CFPHs.

RT-PCR. An RNeasy Tissue Kit (Qiagen, Valencia, CA) was used to isolate total RNA from freeze-thawed 9MM and 10YF PHs, cells of the *h*-hepatoma cell line HepG2, and 12YM and 16YF CFPHs (p = 4). RNA was also isolated with Isogen (Nippon Gene, Tokyo, Japan) from the livers of homozygous uPA/SCID mice and mice chimeric for 12YM PHs or 12YM CFPHs. Each RNA sample was treated with deoxyribonuclease (Takara Bio, Kyoto, Japan) and used as the template for RT-PCR. The RNA (1 μg) was reverse-transcribed with random hexamers using PowerScript Reverse Transcriptase (Clontech, Kyoto, Japan). All reactions were performed with Ex Taq (Takara Bio). Semiquantitative PCR was performed to allow linear amplification of the targets. The following *h*-specific or *m* and *h* cross-reactive genes were subjected to RT-PCR under the conditions shown in Supplementary Table 1: ALB, α1-antitrypsin (AAT), tryptophan-2,3-dioxygenase (TO), glucose-6-phosphatase (G6P), α-fetoprotein (AFP), cytokeratin 19 (CK19), biliary glycoprotein (BGP), Thy-1, CD44, multidrug resistance protein 1 (MDR1), multidrug resistance-associated protein 1 (MRP1), MRP2, and glyceraldehyde-3-phosphate dehydrogenase.

In Situ *Hybridization.* Cryosections (7 μm thick) were fixed with 4% paraformaldehyde, then incubated with 100 ng/mL proteinase K for 10 minutes at 37°C. The sections were then treated at 90°C for 6 minutes and hybridized for 2 hours at 37°C with biotinylated h-DNA probes (Dako, Glostrup, Denmark). The sections were also used to detect whole *h*-genomic DNA using the GenPoint System (Dako) according to the manufacturer's instructions. Finally, they were stained with hematoxylin-eosin.

Immunohistochemistry and Histochemistry. Formalin-fixed livers were embedded in paraffin and sectioned 5 μm thick. The sections were heated in a microwave oven for 5 minutes in Target Retrieval Solution (Dako), then placed at room temperature for 20 minutes. The livers used to generate frozen sections were embedded in OCT compound (Sakura Finechemicals, Tokyo, Japan), frozen in liquid nitrogen, and sectioned 5 μm thick. The cultured cells were fixed in cold ethanol for 10 minutes. The primary antibodies and conditions used for immunohistochemistry are listed in Supplementary Table 2. For bright-field immunohistochemistry, the antibodies were visualized using a Vectastain ABC Kit (Vector Laboratories, Burlingame, CA) using DAB substrates. Fluorescense immunohistochemistry was performed using Alexa 488–conjugated or Alexa 594–conjugated secondary antibodies (Molecular Probes). The nuclei were stained with Hoechst 33258. Glycogens were visualized using a periodic acid-Schiff (PAS) staining kit (Muto Pure Chemicals, Tokyo, Japan). RIs were determined using

*h*ALB-immunostained sections of chimeric *m*-livers as reported previously.[5]

HBV Infection. We obtained *h*-serum containing high-titer HBV DNA (8.1 $\log_{10}$ genome equivalents/mL serum) from an HBV genotype C carrier after obtaining informed consent. The serum was kept at −80°C until use. Four CFPH-chimeric mice were intravenously injected with 100 μL of the HBV-positive serum 9-12 weeks after transplantation.

HBV Marker Analysis. Hepatitis B surface antigen (HBsAg) was measured using an Architect Analyzer (Abbott, Osaka, Japan). Serum DNA was extracted using a SMITEST EX-R&D Nucleic Acid Extraction Kit (Genome Science Laboratories, Fukushima, Japan). Small amounts of HBV DNA (<300 copies/mL) were detected via nested PCR.[8] If HBV DNA was detected during the initial round of PCR, the copy number was determined via real-time PCR as reported.[8]

Results

***Phenotypes of CFPHs* In Vitro.** We seeded 9MM and 12YM PHs on culture dishes and confirmed that the CFPHs from the 2 donors were similar in morphology and replicative capacity. A small number of the CFPHs (0.01%-0.09% of the seeded PHs) began to replicate after 5 days, and the number of replicating cells gradually increased until colonies appeared at 17 days (Fig. 1A); after 21 days, the cells covered the surface of the dish (Fig. 1B). Most of the seeded PHs were not replicative, and they gradually flattened, acquiring a senescent morphology within 20 days of seeding (Fig. 1A). The CFPHs showed an epithelial cell–like morphology with scant cytoplasm (Fig. 1B), and they retained this appearance during subculture (Fig. 1C). The population doubling time (PDT) of the CFPHs gradually increased as the passage number increased. Up to p = 4, the CFPHs from the young donors replicated with a population doubling time of 170-220 hours; subsequently, the population doubling time increased until the cells finally became senescent.[13]

The expression of several marker genes was compared among PHs, HepG2 cells, and CFPHs (Fig. 1D). In our experience, no significant differences exist in the marker gene expression profiles of PHs among different donors, and the same trend applies to subcultured CFPHs.[13] At p = 4, the CFPHs expressed less ALB and AAT messenger RNA compared with the PHs. The PHs expressed TO and G6P, both of which are markers of mature hepatocytes, whereas the CFPHs did not. CK19, a hepatic progenitor/biliary cell marker, was expressed in both the CFPHs and HepG2 cells, but not in the PHs. BGP, a cell–cell adhesion molecule in epithelium, endothelium, and myeloid cells,[16] was expressed in the PHs and HepG2 cells, but only faintly in the CFPHs. The CFPHs, but not the PHs or HepG2 cells, expressed Thy-1, a hematopoietic/hepatic progenitor cell marker. AFP, a hepatic progenitor/carcinoma cell marker, was only detectable in HepG2 cells. CD44, an SH[17] or oval cell marker,[18] was strongly expressed in CFPHs, but only faintly in PHs and HepG2 cells. PHs and CFPHs faintly expressed MDR1. PHs expressed MRP2, but not MRP1. In contrast, CFPHs expressed MRP1, but not MRP2. A change from MRP2 to MRP1 expression during culture has been reported in rat hepatocytes.[19]

Thy-1 and CD44 expression in CFPHs was assessed via immunocytochemistry (Fig. 1E-F). A few CFPHs were positive for Thy-1 (Fig. 1E), whereas the majority was strongly positive for CD44 (Fig. 1F). Fluorescence-activated cell sorting indicated that a minor population of the CFPHs expressed Thy-1 (Fig. 1G-H), with an occupancy rate of 1%-3% (Fig. 1H). The CFPHs expressed CK7, CK8, CK18, and CK19 in the preconfluent state and became CK7- and CK19-negative in condensed regions postconfluence (data not shown), which is in agreement with our previous findings.[13] Other hepatic stem cell markers such as CD34 and c-kit were undetectable in our CFPHs (data not shown).

Repopulation of CFPHs in uPA/SCID Mouse Liver. We transplanted 12YM CFPHs (p = 4) into 27 homozygous uPA/SCID mice. The serum concentration of *h*ALB was monitored posttransplantation as a measure of the RI of CFPHs (Fig. 2A). Approximately half of the hosts had no or only a small increase in the level of *h*ALB throughout the experimental period. The remaining mice showed a continuous increase in the concentration of *h*ALB, which reached >10 μg/mL after 9 to 10 weeks. Animal 27 showed the greatest increase, reaching 0.7 mg/mL after 10 weeks. The RI of each of the 14 mice in which blood *h*ALB concentration was >8 μg/mL after 9 to 10 weeks was determined by dividing the *h*ALB-positive areas by the entire area measured,[5] and the data were plotted against the corresponding blood *h*ALB concentrations (Fig. 2B). RIs between 0.2% and 27.0% were well correlated with blood *h*ALB concentrations in the 9-728 μg/mL range.

Livers of mice engrafted with the CFPHs were subjected to immunohistochemical staining for *h*ALB (Fig. 3A-D,H) and *in situ* hybridization using *h*-genomic DNA probes (Fig. 3I). *h*ALB-positive cells were visible within 3 weeks posttransplantation as single cells or small clusters consisting of up to 25 cells (Fig. 3A-B). Larger clusters containing 20-450 *h*ALB-positive cells appeared after 9 to 10 weeks (Fig. 3C for animal 2 and Fig. 3D for animals 17 and 27). To detect replicating CFPHs, the mice were

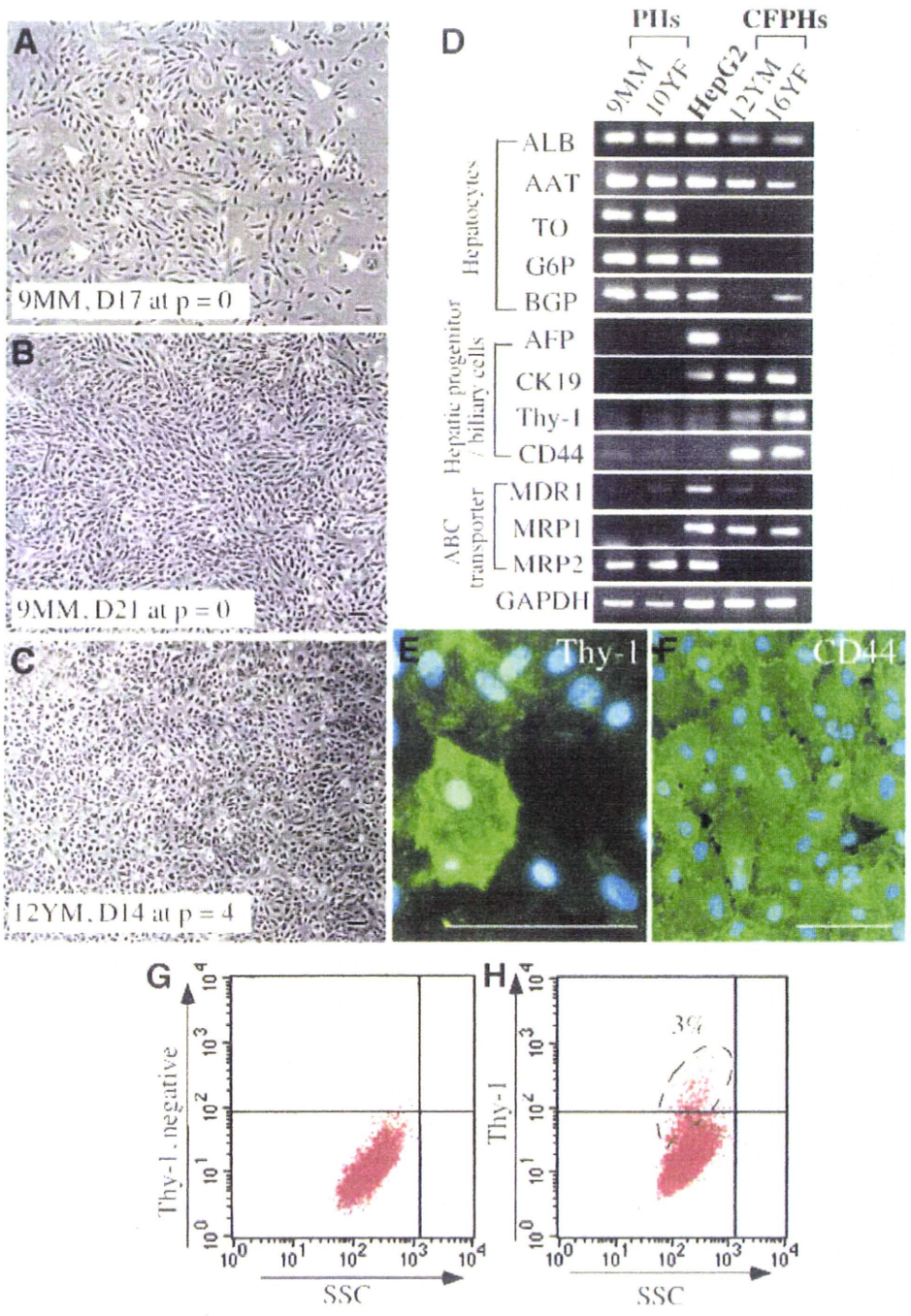

Fig. 1. CFPH growth and gene expression. (A-C) CFPH colony formation. We seeded 9MM PHs at 8×10^3 cells/cm^2 and cocultured with mitomycin C-treated Swiss 3T3 cells in *h*-hepatocyte clonal growth medium. A few CFPHs proliferated and formed colonies. CFPHs were cultured for (A) 17 and (B) 21 days. PHs were nonreplicative and were gradually expelled by replicative CFPHs. Arrowheads indicate the remaining flattened PHs, whose size increased. (C) Cryopreserved 12YM CFPHs (p = 3) were thawed and cultured in *h*-hepatocyte clonal growth medium with Swiss 3T3 cells for 14 days. (D) CFPH messenger RNA expression profiles. RNA was extracted from 9MM and 10YF PHs, HepG2 cells, and 12YM and 16YF CFPHs (p = 4). Semiquantitative RT-PCR was performed for ALB, AAT, TO, G6P, BGP, AFP, CK19, Thy-1, CD44, and the ABC transporters MDR1, MRP1, and MRP2. Glyceraldehyde-3-phosphate dehydrogenase (GAPDH) was used as an internal control. (E,F) Immunohistochemistry of Thy-1 and CD44. 12YM CFPHs (p = 4) were cultured for 14 days and stained for (E) Thy-1 and (F) CD44. The nuclei were stained with Hoechst 33258. Scale bar: 100 μm. (G,H) Flow cytometric analysis of CFPHs for Thy-1. Cells were suspended in Dulbecco's modified Eagle's medium containing 10% fetal bovine serum with (G) *m*-immunoglobulin G_1 as a negative control or (H) anti-*h*Thy-1 antibodies. Living cells were analyzed via fluorescence-activated cell sorting. A small fraction (3% in this case) of the CFPHs was Thy-1$^+$. Three independent analyses were performed with similar results.

given BrdU after 9 weeks. BrdU-positive CFPHs were observed at the edges of the colonies (Fig. 3E-G). Serial liver sections were prepared from CFPH-chimeric mice 9 to 10 weeks after transplantation for *h*ALB immuohistochemistry (Fig. 3H) and for *in situ* hybridization with an *h*-DNA probe (Fig. 3I). The regions identified as containing *h*-hepatocytes by the 2 methods were identical.

Comparison of Repopulation by CFPHs and PHs. PHs and CFPHs (p = 4) were prepared from the livers of 9MM and 12YM donors and transplanted into uPA/SCID mice, and the mice were killed 3 and 10 weeks posttransplantation. The transplanted cells were identified as *h*ALB-positive from histological sections. The number of PH- and CFPH-derived clusters was 125.0 ± 28.2 (n = 3) and 3.3 ± 7.5 (n = 7), respectively, per cross-section of the left lobe of the livers 3 weeks after transplantation, suggesting that the rate of engraftment of the CFPHs was much lower than that of the PHs.

The CFPHs were smaller in size compared with the PHs after 3 weeks (Fig. 4A-B). The cytoplasm of the

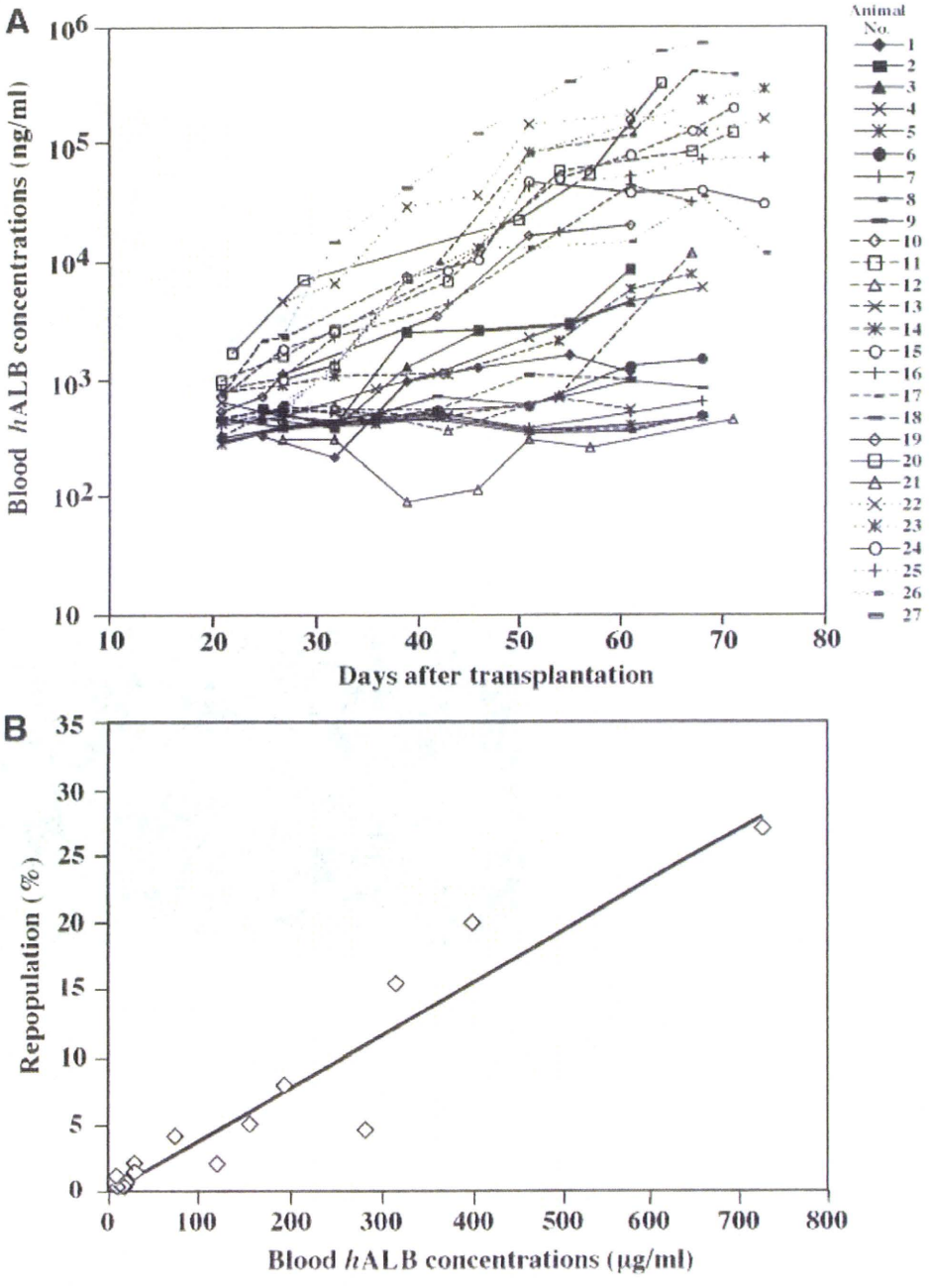

Fig. 2. Transplantation of CFPHs into uPA/SCID mice. The chimeric mice in this experiment are included in group D in Table 1. (A) We transplanted 12YM CFPHs (p = 4) into 27 mice and the serum level of *h*ALB was monitored individually. Ten hosts (animals 1, 5, 6, 7, 8, 9, 10, 13, 18, and 21) did not show significantly elevated *h*ALB levels during the experimental period. Four hosts (2, 3, 4, and 14) showed slight elevation. The *h*ALB concentration of 13 mice (11, 12, 15, 16, 17, 19, 20, 22, 23, 24, 25, 26, and 27) reached >10 μg/mL at 9 to 10 weeks after transplantation. (B) Correlation between the blood *h*ALB level and RI. Fourteen CFPH-chimeric mice (animals 2, 11, 12, 15, 16, 17, 19, 20, 22, 23, 24, 25, 26, and 27) were selected from the mice shown in panel A for RI determination. Their liver sections were immunostained for *h*ALB. RIs were determined for each animal and plotted against the *h*ALB concentration. The correlation coefficient (r^2) between the 2 parameters was 0.91.

former was less abundant and more strongly stained for *h*ALB than that of the latter. We observed *h*CD44 in the plasma membrane of the CFPH-derived cells (Fig. 4E), but not in that of the PH-derived cells (data not shown). At 10 weeks posttransplantation, the CFPHs had increased in size to match those of the PHs, whose sizes were unchanged (Fig. 4C-D), and *h*CD44 expression disappeared from the CFPH-derived cells (Fig. 4F). The diameter of each CFPH and PH was quantified as follows: 18.3 ± 5.1 μm (mean ± SD, n = 65) versus 25.8 ± 6.4 μm (n = 124) at 3 weeks and 27.0 ± 5.5 μm (n = 185) versus 25.8 ± 4.8 μm (n = 187) at 10 weeks. We found no significant differences in this parameter between the 12YM and 9MM samples. Thus, it appears that the CFPHs replicated without changing their original small size until 3 weeks posttransplantation, when they became larger.

Liver sections from the chimeric mice were stained with hematoxylin-eosin to compare the morphological features of PHs and CFPHs at 10 weeks. The repopulated CFPHs (Fig. 4G) showed no significant difference in morphology compared with the repopulated PHs (Fig. 4H). As reported previously,[5,6] the PHs in the chimeric livers were enlarged and had less eosinophilic cytoplasm

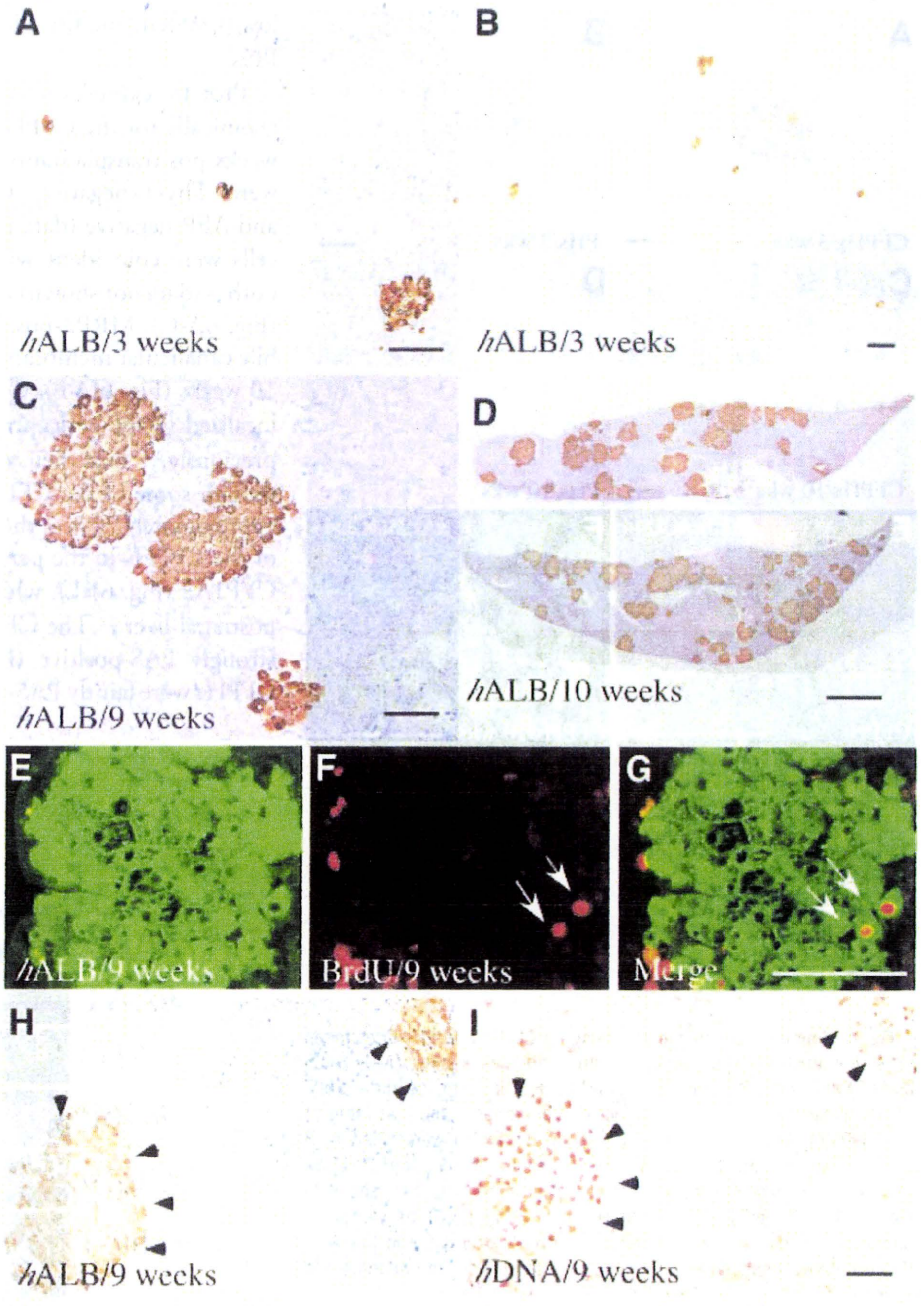

Fig. 3. Engraftment and repopulation of CFPHs in chimeric mouse liver. The chimeric mice in this experiment are included in groups A and D in Table 1. We performed *h*ALB immunohistochemistry using liver sections from CFPH-chimeric mice (A,B) 3, (C) 9, and (D) 10 weeks after transplantation. (A,B) Small clusters composed of 1-25 cells were scattered throughout the liver at 3 weeks in 3 of 9 mice. (C,D) The clusters became larger at 9 to 10 weeks. The liver sections in panel C were prepared from animal 2 in Fig. 2A (RI = 1.1%). The liver sections in panel D were prepared from animals 17 (RI = 20.0%; upper section) and 27 (RI = 27.0%; lower section). Three mice were randomly selected for the BrdU incorporation experiments (animals 2, 19, and 20 in Fig. 2A). They were given BrdU 1 hour before death at 9 weeks posttransplantation. Serial liver sections were subjected to (E) *h*ALB- and (F) BrdU immunohistochemical staining. The image in panel G is panel E and panel F merged. Similar results were obtained from these experiments, and the result from animal 19 (RI = 0.6%) is shown in panels E-G. Serial liver sections were prepared from CFPH-chimeric mice (animals 2, 15, and 17 in Fig. 2A) 9 to 10 weeks after transplantation for *h*ALB immunohistochemistry (H) and for *in situ* hybridization with an *h*-genomic probe (I). Similar results were obtained from the 3 mice. The results shown in panels H and I were obtained from animal 2 (positive cells are indicated by arrowheads). Scale bars in panels A-C, G, and I: 100 μm. Scale bar in panel D: 1 cm.

than the PHs in *h*-livers. The livers of the mice that had low *h*ALB levels at 10 weeks posttransplantation were mostly occupied by red nodules, which have been reported to be formed by the transgene-deleted hepatocytes of the host.[20]

Gene and Protein Expression Profiles of CFPHs in Chimeric Mice Compared with Those of PHs. Three 12YM CFPH-chimeric mice (11, 15, and 17) were randomly selected from the mice in Fig. 2A and killed 10 weeks after transplantation. RNA was extracted from each liver to generate gene expression profiles via RT-PCR. RT-PCR was also performed on 2 12YM PH-chimeric mice that were included in a previous study.[5] The CFPH livers expressed *h*ALB, *h*AAT, *h*TO, *h*G6P, and *h*MRP2, but not *h*CK19, *h*Thy-1, or *h*MRP1, just as in the PH-livers (Fig. 5). Previously, we showed that the PHs in chimeric mice expressed various *h*-cytochrome P450 (*h*CYP) subtypes in a manner similar to the donor liver.[5] In this study, we found that the expression of *h*CYPs 1A2, 2C8, 2C9, 2D6, and 2E1, but not 3A4, in the CFPH-chimeric mice was similar to that in the PH-chimeric mice (data not shown). Expression of *h*CYP3A4 was very

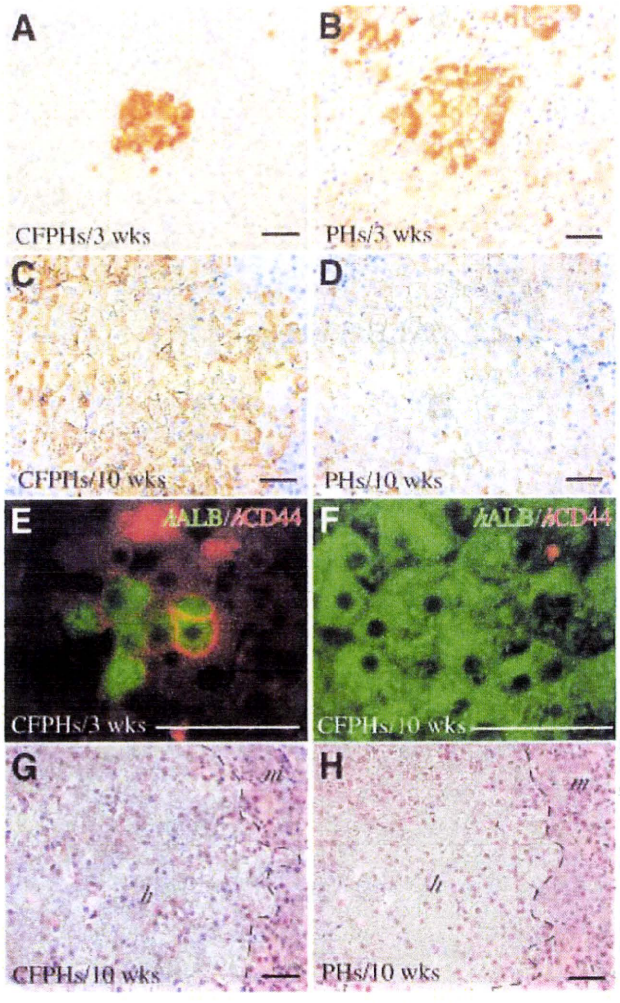

Fig. 4. Immunohistochemical staining for CFPHs and PHs in chimeric mice. Immunohistological analysis with antibodies against (A-D) *h*ALB and (E-F) *h*CD44. We produced 3 12YM CFPH-chimeric mice and 4 9MM CFPH-chimeric mice [(A) and (E), included in groups A and B in Table 1] and 3 9MM PH-chimeric mice [(B), group C], which were killed at 3 weeks posttransplantation. At 10 weeks posttransplantation, 3 12YM CFPH-chimeric mice that were randomly selected from the mice shown in Fig. 2A (15, 16, and 17) were killed [(C) and (F), group D), as were 9MM and 12YM PH-chimeric mice, 2 mice each [(D), groups E and F]. (A-D) Representative images of liver sections prepared from the animals and stained with anti-*h*ALB antibodies. The diameters of the *h*ALB-positive cells were measured in 10-15 randomly selected fields. (E,F) Double-fluorescence immunostaining. Green and red stains depict *h*ALB and *h*CD44, respectively. (G,H) Hematoxylin-eosin staining. (G) Eight CFPH mice were randomly selected from the mice shown in Fig. 2A and killed at 10 weeks posttransplantation. Their liver tissues were then subjected to hematoxylin-eosin staining. (H) Three 12YM PH-chimeric mice were killed at 10 weeks posttransplantation for hematoxylin-eosin staining as above. Similar results were obtained for the 8 CFPH-chimeric mice and 3 PH-chimeric mice. (E-F) Sections from (E) a CFPH-chimeric mouse (RI = 20.0%) and (F) a PH-chimeric mouse (RI = 57%). *h*, *h*-hepatocyte region; *m*, *m*-hepatocyte region. Dashed lines show the boundary between the 2 regions. Scale bars: 50 μm.

low (less than one-fifth) in CFPHs compared with that in PHs.

Protein expression was investigated immunohistochemically for the CFPH-chimeric livers at 3, 9, and 10 weeks posttransplantation. All of the examined CFPHs were Thy-1–negative, CK7-negative, CK19-negative, and AFP-negative (data not shown). The *h*ALB-positive cells were coincident with the *h*CK18-positive cells at both 3 (data not shown) and 9 weeks posttransplantation (Fig. 6A-C). MRP2-positive signals were present on the bile canalicular membranes of the transplanted CFPHs at 10 weeks (Fig. 6D-F). CYP3A4-expressing CFPHs were localized in the pericentral zone (Fig. 6G-I) as reported previously,[21] but their distributions were unique. Although some of the CFPHs were positive for CYP3A4, approximately 70% of them were negative. In contrast, all of the CFPHs in the pericentral zone strongly expressed CYP1A2 (Fig. 6J-L), which is known to be expressed in postnatal liver.[22] The CFPHs in the chimeric mice were strongly PAS-positive (Fig. 6N), whereas the *in vitro* CFPHs were faintly PAS-positive (data not shown). From

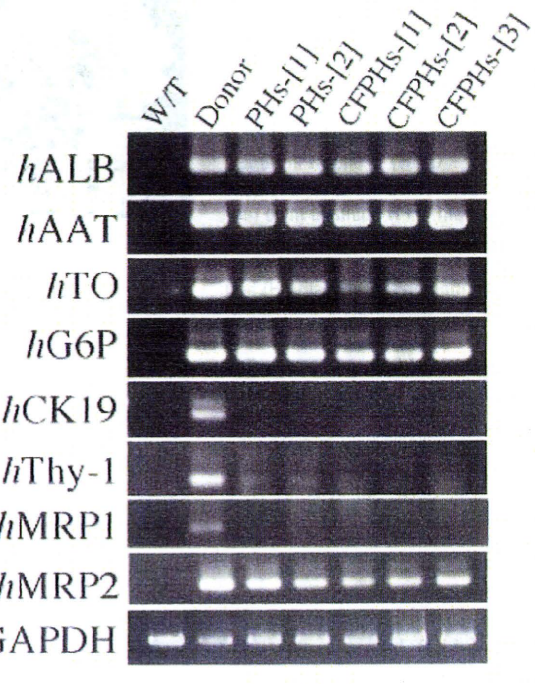

Fig. 5. Gene expression profiles of CFPHs in chimeric mice. Two uPA/SCID mice were transplanted with 12YM PHs ([1] and [2]); 3 uPA/SCID mice were transplanted with 12YM CFPHs ([1], [2], and [3]). The chimeric mice in this experiment are included in groups D and F in Table 1. After 10 weeks, the livers were removed for RT-PCR analysis. At the time of death, the PH-[1]-, PH-[2]-, CFPH-[1]-, CFPH-[2]-, and CFPH-[3]-chimeric mice had RIs of 41.0%, 57.0%, 2.1%, 7.9%, and 20.0%, respectively. The analysis was repeated using liver tissues from donor and uPA/SCID mice without transplantation (W/T). Glyceraldehyde-3-phosphate dehydrogenase (GAPDH) amplification was used as an internal control.

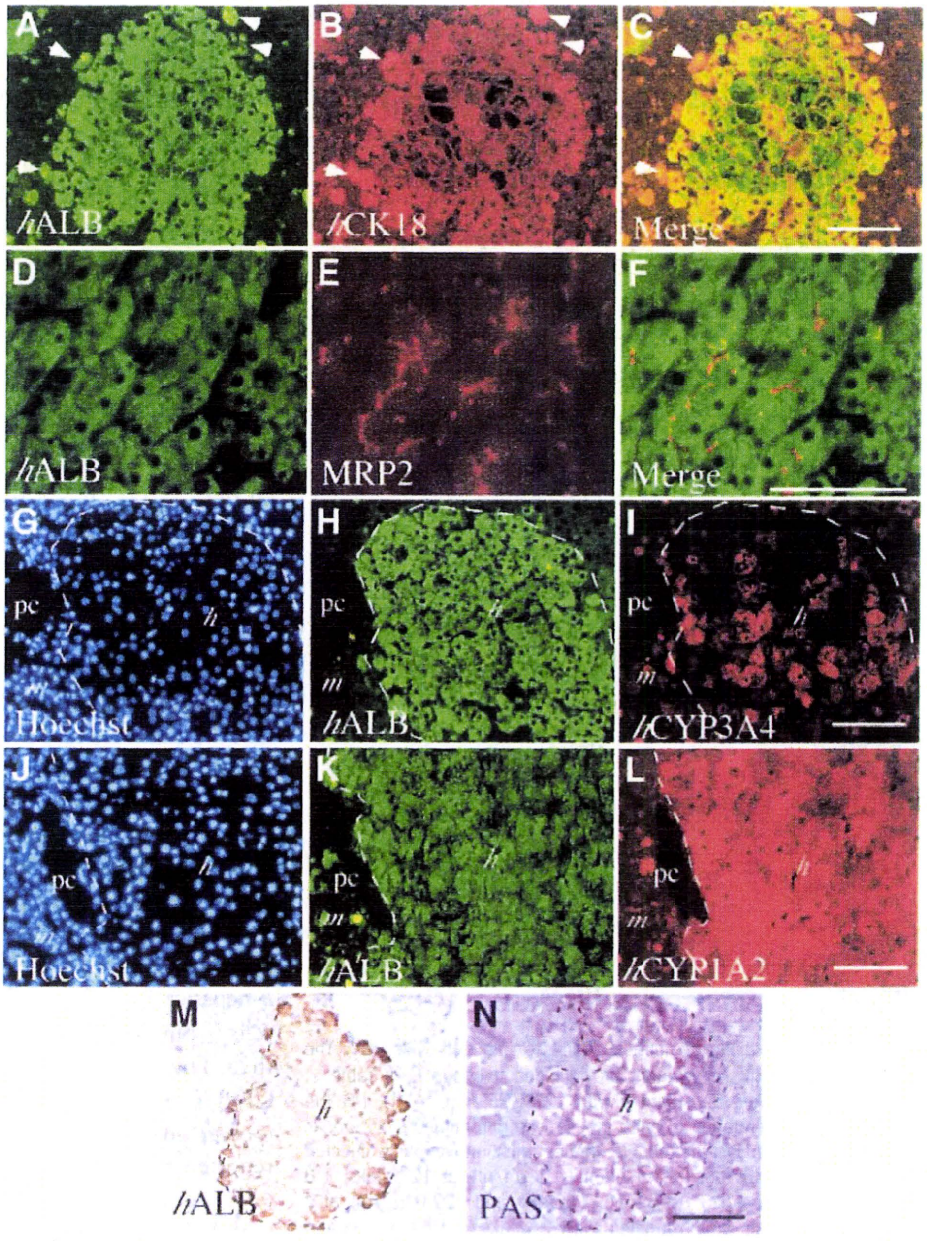

Fig. 6. Protein expression profiles of the CFPHs in chimeric livers. Mice were transplanted with 12YM CFPHs, and their livers were removed 9 to 10 weeks after transplantation for immunohistochemical analysis of (A,D,H,K) *h*ALB, (B) *h*CK18, (E) MRP2, (I) CYP3A4, and (L) CYP1A2. The chimeric mice in this experiment are included in group D in Table 1. Representative images are shown. (A-F) Double-fluorescence immunostaining. (A,D) *h*ALB is stained green. (B) *h*CK18 and (E) *h*MRP2 are stained red. Panels A and B were merged to create panel C; panels D and E were merged to create panel F. The arrowheads in panels A-C show macrophages engulfing such wastes as lipids. Serial sections of liver tissues subjected to 2 series of immunohistochemical examinations, one for (G-I) *h*CYP3A4 and the other for (J-L) *h*CYP1A2. The sections were stained with (G,J) Hoechst 33258, and for (H,K) *h*ALB, (I) *h*CYP3A4, and (L) *h*CYP1A2. Serial sections of liver tissues at 9 weeks posttransplantation were subjected to *h*ALB-immunostaining (M) and PAS staining (N). The positive cells appear brown in (M) and red in (N). *h*, *h*-hepatocyte region; *m*, *m*-hepatocyte region; pc, pericentral zone. Dashed lines show the boundary between the *h*-hepatocyte and *m*-hepatocyte regions. Scale bars: 100 μm.

these results, we conclude that the transplanted CFPHs differentiated into functionally mature hepatocytes. No *h*-cell tumors were formed during any of our experiments in the uPA/SCID mice.

Infection of CFPH-Chimeric Mice with HBV. To further examine whether CFPHs had exhibited normal differentiated phenotypes in chimeric mice, we tested their susceptibility to HBV infection. Four CFPH-chimeric mice with various serum *h*ALB levels (0.2, 1.6, 7.3, and 222.0 μg/mL) were inoculated with 100 μL of HBV-positive *h*-serum at 9-12 weeks posttransplantation. The animals were then tested every 2 weeks for HBV viremia and serum *h*ALB levels (Fig. 7A). The amount of HBV DNA in the animals increased between 2 and 8 weeks after inoculation, and all 4 mice developed measurable viremia within 8 weeks. However, a correlation was observed between the HBV DNA and/or HBsAg level and the *h*ALB level: the former appeared to be high when the latter was high (Fig. 7A). HBsAg was detectable in the serum of the chimeric mice when they showed elevated virus titers: the HBsAg levels of chimeric mice with HBV DNA levels of 2×10^3, 5.2×10^5, 5.9×10^7, and 7.7×10^8 copies/mL 8 weeks after inoculation were <0.05, <0.05, 3.2, and 124.0 IU/mL, respectively. HBV was infectious to CFPH-chimeric mice with very low levels of *h*ALB ($<10^4$ ng/mL), and all mice showed quantitatively

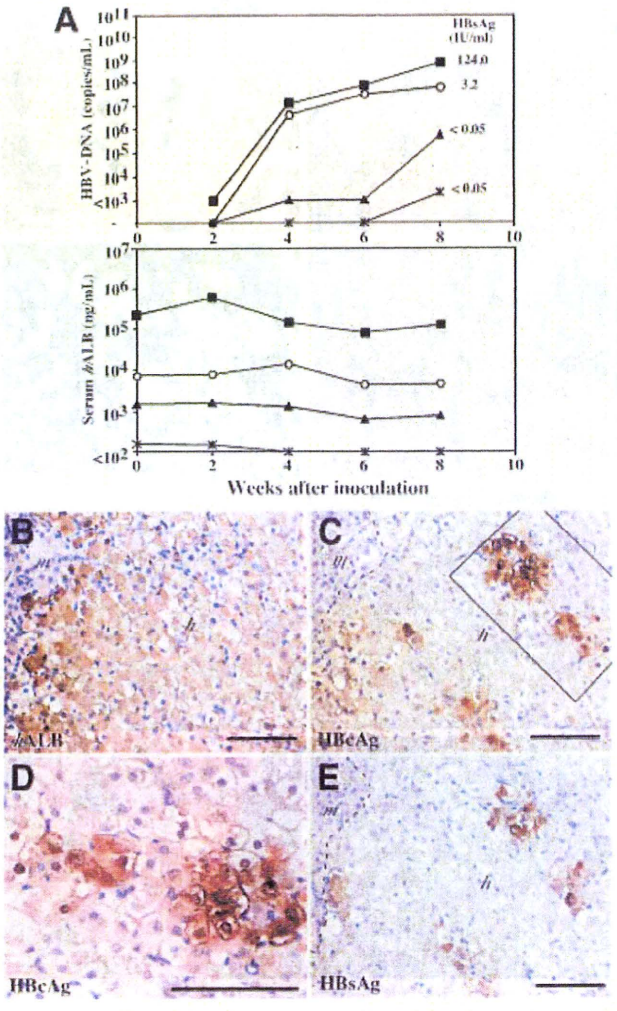

Fig. 7. Susceptibility of chimeric mice to infection with HBV. The chimeric mice in this experiment are included in group G in Table 1. uPA/SCID mice were transplanted with 12YM CFPH (p = 4). (A) The serum *h*ALB concentration of each mouse was determined 9-12 weeks posttransplantation just before the mouse was intravenously injected with 100 μL of HBV-positive *h*-serum (0.2 μg/mL at 12 weeks, 1.6 μg/mL at 10 weeks, 7.3 μg/mL at 11 weeks, and 222.0 μg/mL at 9 weeks). The animals were examined every 2 weeks for HBV viremia and serum *h*ALB level. The upper and lower graphs show the HBV DNA levels (copies/mL) and serum *h*ALB concentrations (ng/mL), respectively. The amount of HBV DNA ($<10^3$ copies/mL) was semiquantitatively measured via nested PCR. The values in the upper graph represent the HBsAg levels at 8 weeks. (B-E) Immunohistochemical analysis of chimeric livers infected with HBV. Serial sections of liver tissues at 8 weeks after inoculation were stained for (B) *h*ALB, (C,D) hepatitis B core antigen, and (E) HBsAg. The region enclosed by a square in panel C is magnified in panel D. Scale bars: 100 μm.

measurable viremia ($>10^3$ copies/mL) up to 8 weeks after inoculation. In contrast, most PH-chimeric mice with $<10^4$ ng/mL *h*ALB did not show quantitatively measurable levels of viremia up to 12 weeks after inoculation (data not shown) as reported previously.[8] In this study, we confirmed that CFPHs were not susceptible to infection with HBV prior to transplantation. The presence of hepatitis B core antigen and HBsAg in the CFPHs from HBV-infected chimeric livers was examined immunohistochemically (Fig. 7C,E). CFPHs were positive for both antigens that were sporadically distributed in the same regions among the CFPH colonies. Hepatitis B core antigen–positive cells accounted for 18.7 ± 8.3% of the total number of CFPHs (n = 3; total cell count = 1,215) (Fig. 7C), and both the nucleus and cytoplasm of the cells showed signals (Fig. 7D).

Discussion

This study supports our previous conclusion that CFPHs are *h*-hepatic progenitor-like cells.[13] Cultured CFPHs expressed such hepatic progenitor cell markers as CK19, Thy-1, and CD44, but not mature hepatocyte markers such as TO and G6P. We also found that *in vitro*–expanded CFPHs in uPA/SCID mice were able to repopulate the parenchyma, in which they differentiated into mature hepatocytes. FISH (fluorescence *in situ* hybridization) using mouse X chromosome probes showed that the engrafted and propagated CFPHs did not fuse to the mouse cells (data not shown). Thus, replicative CFPHs isolated from postnatal liver are normal, functional hepatocyte progenitor-like cells.

The existence of stem/progenitor cells in the adult liver is controversial.[23-25] In the present study, we showed that the CFPHs expressed CK19, Thy-1, and CD44, but not AFP, in serial culture. Thy-1 antigens are expressed in *h*-hepatic progenitor cells in fetal liver[26] and in rat oval cells,[27] but not in normal adult hepatocytes. We showed that Thy-1-expressing cells were present among the CFPHs at an occupancy of 1%-3%. SHs show greater growth potential than PHs in rats.[12] Other studies have reported that CD44 is a specific marker for rat SHs *in vitro* and *in vivo*, and that its expression level decreases with SH maturation *in vitro*.[17] Moreover, a recent study demonstrated that CD44 was strongly expressed by oval cells in a 2-acetylaminofluorene/partial hepatectomy, a D-galactosamine, and a retrorsine/partial hepatectomy rat model, but not by small hepatocyte-like progenitor cells (SHPCs)[18] that appeared in a retrorsine/partial hepatectomy model.[28] We detected CD44 expression in CFPHs at the plasma membrane. These results suggest that Thy-1 and CD44 may be common markers for both rat and *h*-hepatic progenitor cells.

Mouse embryonic liver stem cell lines differentiate into both hepatocytes and bile ducts in uPA/SCID mice.[29] Like PHs, our CFPHs differentiated into mature hepatocytes, but not into biliary epithelial cells, in uPA/SCID mice. CFPHs are considered to be hepatic progenitor-like cells, like rat SHs[12,30-33] and SHPCs.[28,34] SHPCs are

closely related to SHs; they are small and similar in size,[28,30] and both express CYP3A1 and 2E1 at a low level.[28,32] At 3 weeks posttransplantation, the CFPHs were small in size, had a large nucleus-to-cytoplasm ratio, and expressed *h*CD44, but not *h*CK19. At 10 weeks, the cells became bigger, assumed a morphology similar to that of PH-derived cells, and lost their expression of *h*CD44. The expression of *h*CYP3A4 was quite low (0.15-fold) among CFPHs compared with that of PHs (data not shown). In addition, the distribution of *h*CYP3A4-expressing CFPHs in the pericentral zone was unique: more than two-thirds of CFPHs did not express CYP3A4. In the case of the *h*-PH–chimeric mice, all PHs in the pericentral zone expressed CYP3A4 (data not shown).

Presently, we lack experimental data to explain the expression of *h*CYP3A4 in CFPH-chimeric liver, but CFPHs may require some specific environmental factor(s) for differentiation, which might be absent from mouse liver. Alternatively, some factors that specifically inhibit the differentiation of CFPHs might be present there. CK7-positive *h*-hepatic progenitor cells are present in the livers of uPA/SCID mice transplanted with *h*-postnatal liver-derived PHs,[6] and these small cells are strongly immunoreactive to pan-cytokeratin with scant cytoplasm. The CFPHs were morphologically similar to these cells at 3 weeks posttransplantation, although we were unable to detect CK7-positive cells in either the PH- or CFPH-transplanted chimeric livers. However, CFPHs were *h*CK7-, *h*CK19-, and *h*CD44-positive, at least until 1 day posttransplantation (data not shown).

We reported previously that uPA/SCID livers were nearly completely replaced with young donor PHs at 10 weeks posttransplantation.[5] In contrast, the RIs of our CFPH-chimeric mice were <30% at 9 to 10 weeks. CFPHs were rare in the host liver at 3 weeks posttransplantation, whereas several PHs were observed. The lower RIs of the CFPHs might be attributable to their lower engraftment efficiency.

In conclusion, *h*-hepatocytes in immunodeficient, and liver-injured mice are useful for the study of viral hepatitis. Repopulated *h*-hepatocytes are susceptible to infection with HBV[6-8] and HCV.[4,6] Additionally, *h*-hepatocyte–chimeric mice are usually produced by transplanting fresh[6,7] or cryopreserved hepatocytes,[4,5] but sources of *h*-hepatocytes are limited. Several studies have reported on liver repopulation by *in vitro*–propagated cells from adult and fetal livers, such as immortalized mouse hepatic stem cells,[29] rat SHPCs,[34] immortalized *h*-hepatocytes transfected with full-length HBV,[35] and fetal *h*-epithelial/hepatic progenitor cells.[36,37] However, the RIs in these studies were extremely low (less than a few percent). In the present study, we were able to produce CFPH-chimeric mice with RIs as high as 27%. Thus, CFPHs could be an alternative to *h*-hepatocytes as a source of hepatocytes for transplantation. Moreover, the CFPH-chimeric mice were susceptible to infection with HBV, even though their serum *h*ALB levels were extremely low (10^2-10^3 ng/mL). CFPH-chimeric mice will be useful for studying *h*-HBV and for characterizing *h*-hepatic progenitor cells.

Acknowledgment: We thank H. Kohno, Y. Matsumoto, S. Nagai, A. Tachibana, Y. Yoshizane, and Y. Seo for providing technical assistance. We also thank Dr. K. Ohashi (Tokyo Women's Medical University) for helpful discussion and comments during the preparation of this manuscript.

References

1. Rhim JA, Sandgren EP, Degen JL, Palmiter RD, Brinster RL. Replacement of diseased mouse liver by hepatic cell transplantation. Science 1994; 263:1149-1152.
2. Overturf K, Al-Dhalimy M, Ou CN, Finegold M, Grompe M. Serial transplantation reveals the stem-cell-like regenerative potential of adult mouse hepatocytes. Am J Pathol 1997;151:1273-1280.
3. Laconi E, Oren R, Mukhopadhyay DK, Hurston E, Laconi S, Pani P, et al. Long-term, near-total liver replacement by transplantation of isolated hepatocytes in rats treated with retrorsine. Am J Pathol 1998;153:319-329.
4. Mercer DF, Schiller DE, Elliott JF, Douglas DN, Hao C, Rinfret A, et al. Hepatitis C virus replication in mice with chimeric human livers. Nat Med 2001;7:927-933.
5. Tateno C, Yoshizane Y, Saito N, Kataoka M, Utoh R, Yamasaki C, et al. Near completely humanized liver in mice shows human-type metabolic responses to drugs. Am J Pathol 2004;165:901-912.
6. Meuleman P, Libbrecht L, De Vos R, de Hemptinne B, Gevaert K, Vandekerckhove J, et al. Morphological and biochemical characterization of a human liver in a uPA-SCID mouse chimera. HEPATOLOGY 2005;41: 847-856.
7. Dandri M, Burda MR, Török E, Pollok JM, Iwanska A, Sommer G, et al. Repopulation of mouse liver with human hepatocytes and *in vivo* infection with hepatitis B virus. HEPATOLOGY 2001;33:981-988.
8. Tsuge M, Hiraga N, Takaishi H, Noguchi C, Oga H, Imamura M, et al. Infection of human hepatocyte chimeric mouse with genetically engineered hepatitis B virus. HEPATOLOGY 2005;42:1046-1054.
9. Kocarek TA, Schuetz EG, Guzelian PS. Biphasic regulation of cytochrome P450 2B1/2 mRNA expression by dexamethasone in primary cultures of adult rat hepatocytes maintained on matrigel. Biochem Pharmacol 1994; 48:1815-1822.
10. Arterburn LM, Zurlo J, Yager JD, Overton RM, Heifetz AH. A morphological study of differentiated hepatocytes *in vitro*. HEPATOLOGY 1995;22: 175-187.
11. Tateno C, Yoshizato K. Growth and differentiation in culture of clonogenic hepatocytes that express both phenotypes of hepatocytes and biliary epithelial cells. Am J Pathol 1996;149:1593-1605.
12. Tateno C, Takai-Kajihara K, Yamasaki C, Sato H, Yoshizato K. Heterogeneity of growth potential of adult rat hepatocytes *in vitro*. HEPATOLOGY 2000;31:65-74.
13. Yamasaki C, Tateno C, Aratani A, Ohnishi C, Katayama S, Kohashi T, et al. Growth and differentiation of colony-forming human hepatocytes *in vitro*. J Hepatol 2006;44:749-757.
14. Hino H, Tateno C, Sato H, Yamasaki C, Katayama S, Kohashi T, et al. A long-term culture of human hepatocytes which show a high growth poten-

tial and express their differentiated phenotypes. Biochem Biophys Res Commun 1999;256:184-191.
15. Kocken, JM, de Heer E, Borel Rinkes IH, Sinaasappel M, Terpstra OT, Bruijn JA. Blocking of $\alpha 1\beta 1$ integrin strongly improves survival of hepatocytes in allogeneic transplantation. Lab Invest 1997;77:19-28.
16. Prall F, Nollau P, Neumaier M, Haubeck HD, Drzeniek Z, Helmchen U, et al. CD66a (BGP), an adhesion molecule of the carcinoembryonic antigen family, is expressed in epithelium, endothelium, and myeloid cells in a wide range of normal human tissues. J Histochem Cytochem 1996;44:35-41.
17. Kon J, Ooe H, Oshima H, Kikkawa Y, Mitaka T. Expression of CD44 in rat hepatic progenitor cells. J Hepatol 2006;45:90-98.
18. Yovchev MI, Grozdanov PN, Joseph B, Gupta S, Dabeva MD. Novel hepatic progenitor cell surface markers in the adult rat liver. HEPATOLOGY 2007;45:139-149.
19. Rippin SJ, Hagenbuch B, Meier PJ, Stieger B. Cholestatic expression pattern of sinusoidal and canalicular organic anion transport systems in primary cultured rat hepatocytes. HEPATOLOGY 2001;33:776-782.
20. Sandgren EP, Palmiter RD, Heckel JL, Daugherty CC, Brinster RL, Degen JL. Complete hepatic regeneration after somatic deletion of an albumin-plasminogen activator transgene. Cell 1991;66:245-256.
21. Oinonen T, Lindros KO. Hormonal regulation of the zonated expression of cytochrome P-450 3A in rat liver. Biochem J 1995;309:55-61.
22. Sonnier M, Cresteil T. Delayed ontogenesis of CYP1A2 in the human liver. Eur J Biochem 1998;251:893-898.
23. Sell S. Is there a liver stem cell? Cancer Res 1990;50:3811-3815.
24. Thorgeirsson SS. Hepatic stem cells. Am J Pathol 1993;142:1331-1333.
25. Shafritz DA, Oertel M, Menthena A, Nierhoff D, Dabeva MD. Liver stem cells and prospects for liver reconstitution by transplanted cells. HEPATOLOGY 2006;43(Suppl):89S-98S.
26. Masson NM, Currie IS, Terrace JD, Garden OJ, Parks RW, Ross JA. Hepatic progenitor cells in human fetal liver express the oval cell marker Thy-1. Am J Physiol Gastrointest Liver Physiol 2006;291:G45-G54.
27. Petersen BE, Goff JP, Greenberger JS, Michalopoulos GK. Hepatic oval cells express the hematopoietic stem cell marker Thy-1 in the rat. HEPATOLOGY 1998;27:433-445.
28. Gordon GJ, Coleman WB, Grisham JW. Temporal analysis of hepatocyte differentiation by small hepatocyte-like progenitor cells during liver regeneration in retrorsine-exposed rats. Am J Pathol 2000;157:771-786.
29. Strick-Marchand H, Morosan S, Charneau P, Kremsdorf D, Weiss MC. Bipotential mouse embryonic liver stem cell lines contribute to liver regeneration and differentiate as bile ducts and hepatocytes. Proc Natl Acad Sci U S A 2004;101:8360-8365.
30. Katayama S, Tateno C, Asahara T, Yoshizato K. Size-dependent *in vivo* growth potential of adult rat hepatocytes. Am J Pathol 2001;158:97-105.
31. Mitaka T, Mikami M, Sattler GL, Pitot HC, Mochizuki Y. Small cell colonies appear in the primary culture of adult rat hepatocytes in the presence of nicotinamide and epidermal growth factor. HEPATOLOGY 1992;16:440-447.
32. Asahina K, Shiokawa M, Ueki T, Yamasaki C, Aratani A, Tateno C, et al. Multiplicative mononuclear small hepatocytes in adult rat liver: their isolation as a homogeneous population and localization to periportal zone. Biochem Biophys Res Commun 2006;342:1160-1167.
33. Yoshizato K. Growth potential of adult hepatocytes in mammals: highly replicative small hepatocytes with liver progenitor-like traits. Dev Growth Differ 2007;49:171-184.
34. Gordon GJ, Butz GM, Grisham JW, Coleman WB. Isolation, short-term culture, and transplantation of small hepatocyte-like progenitor cells from retrorsine-exposed rats. Transplantation 2002;73:1236-1243.
35. Brown JJ, Parashar B, Moshage H, Tanaka KE, Engelhardt D, Rabbani E, et al. A long-term hepatitis B viremia model generated by transplanting nontumorigenic immortalized human hepatocytes in Rag-2-deficient mice. HEPATOLOGY 2000;31:173-181.
36. Malhi H, Irani AN, Gagandeep S, Gupta S. Isolation of human progenitor liver epithelial cells with extensive replication capacity and differentiation into mature hepatocytes. J Cell Sci 2002;115:2679-2688.
37. Nowak G, Ericzon BG, Nava S, Jaksch M, Westgren M, Sumitran-Holgersson S. Identification of expandable human hepatic progenitors which differentiate into mature hepatic cells *in vivo*. Gut 2005;54:972-979.

doi:10.1111/j.1440-1746.2007.05036.x

HEPATOLOGY

Immunological role of indoleamine 2,3-dioxygenase in rat liver allograft rejection and tolerance

Yu-Chun Lin,*† Chao-Long Chen,† Toshiaki Nakano,† Shigeru Goto,†‡ Ying-Hsien Kao,† Li-Wen Hsu,† Chia-Yun Lai,† Bruno Jawan,§ Yu-Fan Cheng,¶ Chise Tateno** and Katsutoshi Yoshizato*

*Department of Biological Science, Developmental Biology Laboratory, Graduate School of Science, Hiroshima University, **Japan Science and Technology Corporation, Hiroshima Prefectural Institute of, Industrial Science and Technology, Hiroshima, †Iwao Hospital, Oita, Japan; Liver Transplantation Program and Departments of ‡Surgery, §Anesthesiology, and ¶Diagnostic Radiology, Kaohsiung Chang Gung Memorial Hospital, Kaohsiung, Taiwan

Key words
indoleamine 2,3-dioxygenase, liver transplantation, parenchymal cell, rejection, tolerance.

Accepted for publication 1 February 2007.

Correspondence
Dr Yu-Chun Lin, Liver Transplantation Program, Kaohsiung Chang Gung Memorial Hospital, 123 Ta-Pei Rd, Niao-Sung Hsiang, Kaohsiung 83305, Taiwan. Email: kcgmh.livertx@msa.hinet.net

Abstract

Background and Aim: Indoleamine 2,3-dioxygenase (IDO) is expressed in the placenta and plays an essential role in maternal tolerance. Recent data showed that giving IDO inhibitor blocked liver allograft tolerance. However, the immunological role of IDO in rat liver allograft models has not been characterized. In the present study, the time-course of IDO expression and the localization of IDO were analyzed to address the role of IDO in the induction of tolerance.

Methods: Rat orthotopic liver transplantations (OLT) were performed and *IDO* gene expression of OLT livers was analyzed. Immunohistochemistry was used to evaluate the localization of IDO-expressed cells in the liver.

Results: The *IDO* gene was detected in the allogeneic liver graft at the acute phase but the signal could not be detected when these OLT rats were treated with cyclosporince A. The time-course of *IDO* gene expression in liver grafts of the spontaneous tolerant OLT model revealed that the IDO mRNA was expressed in both the rejection phase and the induction phase of tolerance, but the signal was gradually lowered during the maintenance phase of tolerance. Immunohistochemistry confirmed that the IDO protein was detected in antigen-presenting cells but not in hepatocytes.

Conclusion: Our results demonstrated that IDO is induced in antigen-presenting cells of rat liver allografts under drug-free status, suggesting that indirect or direct recognition of donor antigen and further T-cell activation may be inhibited. IDO may act as a local immunosuppressive molecule to protect transplanted cells, tissues and organs from immune attack.

Introduction

The immunobiology of liver transplantation has been the subject of much scrutiny since it was recognized that a liver allograft between unrelated individuals can be accepted without immunosuppressive treatment in experimental orthotopic liver transplantation (OLT) models.[1,2] Elucidation of the immune mechanism underlying the acceptance of liver allografts in animal models could lead to the establishment of novel means to promote the acceptance of transplant organs. A number of possible mechanisms and factors have been suggested to contribute to this unique behavior of liver allografts, including the action of soluble class I antigens,[3-5] clonal deletion and anergy.[6-8] However, the mechanisms and the cellular factors involved in this natural liver-related tolerance phenomenon have not been fully translated from animal models to clinical settings.

In a rat OLT model, PVG (MHC haplotype: RT1^c) recipients spontaneously accept livers of DA (RT1^a) in the absence of extra immunosuppressive treatment, whereas other organ allografts in this combination are promptly rejected. Furthermore, PVG recipients that have already accepted DA livers accept other organs from the DA strain but not from a third party strain.[2,3,9] Although this liver-induced donor-specific tolerance has not been confirmed in clinical liver transplantation, we have recently been able to obtain patients who would accept liver allografts after the cessation of immunosuppressive drugs as one of the therapies for post-transplant lymphoproliferative disease (PTLD). In a tolerance rat OLT model or in drug-free OLT patients, we and others have also demonstrated the suppression of graft-versus-host reaction (GVH) by OLT,[10] a normal response of mixed lymphocyte reaction (MLR) against donor antigen,[11] the generation of regulatory cells,[12-14] the existence of the recipient's donor-reactive CD4 T cells,[15] microchimerism established by functional donor-derived cells,[16-20] the presence of liver suppressive factors[21] and the presence of cytokines.[22,23] These findings lead us to support the hypothesis that tolerance or acceptance of a liver allograft depends on the delicate

balance of the immune reaction between host and graft where certain OLT-specific mediators may regulate the immunological reaction from host to graft and also from graft to host.

The absence of a harmful maternal immune response against the fetal allograft during pregnancy is another intriguing model of immune tolerance[24] and may provide many hints about the mechanisms of liver allograft tolerance. Munn *et al.* first suggested that expression of indoleamine 2,3-dioxygenase (IDO), a tryptophan-catalyzing enzyme present in the placenta during pregnancy, is required to prevent rejection of the allogeneic fetus from maternal T cells by generating a tryptophan-deficient environment in the placenta.[25] Indeed, this hypothesis has been supported by other *in vitro* studies that showed that IDO expression by macrophages[26] and dendritic cells (DC)[27] inhibits bystander lymphocyte proliferation. We have also reported that IDO is necessary for natural killer (NK) cells to combat tumor cells.[28,29] In the field of transplantation biology research, the overexpression of IDO in an organ or tissue by the gene delivery protocol prolonged the survival of pancreatic islet cells,[30] skin substitutes,[31] lung[32] and cornea.[33] However, the administration of an IDO inhibitor blocked the tolerance in a mouse OLT model.[34] Thus, IDO appears to be produced to maintain the homeostasis in immunology related to pregnancy, cancer and transplantation, as inhibition of IDO led to abortion of the fetus, proliferation of tumor or rejection of liver allografts, respectively.

In our previous study,[35] we found that gene expression of IDO can be detected in livers after allogeneic liver transplantation but not in the livers of naïve rats. However, the immunological role of the *IDO* gene in rat liver allograft models has not been characterized. In the present study, we examined the time-course of IDO expression together with the discrete localization of IDO synthesis to fully address the immunological role of IDO in rejection and in the induction of tolerance.

Methods

Animals

This project was conducted according to the *Guide for the Care and Use of Laboratory Animals* (Chinese-Taipei Society of Laboratory Animal Sciences) and was approved by our institutional Animal Welfare Committee. Rats were housed under 12:12-h light/dark cycles in specific-pathogen-free animal facilities. The water and commercial rat food were provided ad libitum.

Male DA ($RT1^a$) and PVG ($RT1^c$) rats weighing 200–250 g were obtained from Japan SLC (Hamamatsu, Japan) and the Institute of Laboratory Animals, Graduate School of Medicine, Kyoto University (Kyoto, Japan), respectively. Male LEW ($RT1^l$) rats weighing 200–250 g were obtained from Taiwan National Laboratory Animal Center (Taipei, Taiwan).

Effect of IDO and kynurenine on mixed lymphocyte reaction

Mixed lymphocyte reaction assay was performed as described previously.[36] Briefly, rat splenocytes were harvested and treated with 150 mM NH_4Cl, 15 mM $NaHCO_3$, and 0.1 mM ethylenediaminetetraacetic acid (EDTA; pH 7.3) to lyze the red blood cells. After being washed twice with phosphate-buffered saline (PBS), splenocytes were suspended in RPMI-1640 medium (Invitrogen, Carlsbad, CA, USA) supplemented with 10% fetal calf serum (Invitrogen), 100 U/mL penicillin and 100 μg/mL streptomycin (Invitrogen). Stimulator cells (DA splenocytes; 10^7 cells/mL) were treated with 25 μg/mL mitomycin C (Sigma-Aldrich, St Louis, MO, USA) at 37°C for 30 min to block cell proliferation. Responder PVG cells (5×10^4 cells in 100 μL) were mixed with stimulator cells (5×10^5 cells in 100 μL) in 96-well round-bottom plates and incubated at 37°C for 72 h in a humidified atmosphere of 5% carbon dioxide and 95% air. The MLR culture was then supplemented with IDO (25 μg/mL; ALEXIS Corp., Lausen, Switzerland), IDO with tryptophan (300 μM), IDO with IDO inhibitor (2 nM; 1-methyl-DL-tryptophan, 1-MT) and kynurenine (150 μM) (Sigma-Aldrich) to evaluate their immunological activity. Albumin (25 μg/mL) was used as a control. Allogeneic T-cell response was determined by using the WST-1 kit (Roche Diagnostics, Mannheim, Germany) with an MRX Microplate Reader (Dynex Technologies, Chantilly, VA USA).

Rat OLT and liver samples collection

Orthotopic liver transplantation was performed by the method described by Kamada and Calne.[37] DA livers were orthotopically transplanted into DA, PVG or LEW recipients. As reported previously,[38] OLT (DA-PVG) rats naturally overcome rejection without using any type of immunosuppressants (spontaneous tolerance model). In contrast, all OLT (DA-LEW) rats die from acute rejection within 14 days (acute rejection model). Allograft survival of OLT (DA-LEW) rats was prolonged when they were treated with cyclosporinee A (CsA; 15 mg/kg per day) for 14 days after OLT surgery (drug-induced acceptance model). Syngeneic OLT (DA-DA) rats were used as controls to rule out the surgically inducible factors. The animals of each group were killed at various days after OLT. The livers were cut into pieces and then snap frozen in liquid nitrogen for further experiments. For RNA isolation, the livers were ground into powder in the liquid nitrogen.

Isolation of hepatic constituent cells

Fractions of hepatic constituent cells, which include parenchymal cells (PC) (hepatocytes) and non-parenchymal cells (NPC), were prepared following the procedure described previously.[39] Disaggregated hepatic constituent cells were obtained from OLT rats by the collagenase perfusion technique. In brief, livers were removed after portal vein perfusion with Hanks' balanced salt solution (HBSS; Invitrogen) containing 0.02% ethylene glycol-bis(β-aminoethyl ether)-*N*,*N*,*N*′,*N*′-tetraacetic acid (EGTA; Sigma Aldrich) and HBSS-containing 0.05% collagenase (Wako, Osaka, Japan). Whole hepatic constituent cells were centrifuged twice at 50 *g* for 2 min. The pellet and supernatant were used for the preparation of PC and NPC, respectively. The PC-fraction containing hepatocytes was purified again as a pellet obtained by centrifuging the cell suspension through 45% Percoll (GE Healthcare Bio-Sciences, Piscataway, NJ, USA) at 50 *g* for 24 min. The NPC fraction was centrifuged at 150 *g* twice for 5 min, and the pellet was collected. This pellet was suspended in Dulbecco's modified Eagle's medium (Invitrogen) and centrifuged at 50 *g* for 2 min to eliminate contaminative hepatocytes, and a fraction of the NPC

Table 1 Characteristics of primers and polymerase chain reaction condition

mRNA	Sense primer	Antisense primer	Annealing temperature	Fragment size
IDO	5′-CCTGACTTATGAGAACATGGACGT-3′	5′ATACACCAGACCGTCTGATAGCTG-3′	55°C	321 bp
IFN-γ	5′-CCCTCTCTGGCTGTTACTGC-3′	5′-CTCCTTTTCCGCTTCCTTAG-3′	60°C	419 bp
TDO	5′-GAGCAGGAGCAGACGCTATT-3′	5′-CACCTTGTACCTGTCGCTCA-3′	55°C	498 bp
β-actin	5′-CGACGAGGCCCAGAGCAAGAGA-3′	5′-CCAGGGCGACGTAGCACAGCTT-3′	60°C	500 bp

IDO, indoleamine 2,3-dioxygenase; IFN, interferon; TDO, TDO, tryptophan 2,3-dioxygenase.

was obtained as a supernatant. These PC and NPC fractions were used for RNA isolation and reverse transcription–polymerase chain reaction (RT-PCR) assay.

RNA isolation and RT-PCR assay

Total RNA was isolated from liver grafts, hepatocytes or the NPC fraction by using the Trizol reagent (Invitrogen), following the manufacturer's instructions. The cDNA was synthesized from total RNA (2 μg) with oligo-dT primer and ImProm-II reverse transcriptase (Promega Biosciences, Madison, WI, USA). The RT reaction mixture was incubated at 42°C for 90 min, and the reaction was terminated by heating at 90°C for 10 min, followed by rapid chilling on ice for 5 min. PCR was carried out using IDO, interferon (IFN)-γ, tryptophan 2,3-dioxygenase (TDO) and β-actin (Table 1). The housekeeping β-actin mRNA was used as a loading control. The PCR was conducted with 27 cycles for β-actin and TDO, and 35 cycles for IDO and IFN-γ. PCR products were separated by electrophoresis in 2% agarose gels and stained with ethidium bromide, and the bands were visualized under ultraviolet light.

Immunostaining of the OLT-liver section

All tissues examined by immunostaining were embedded into the Tissue-Tek® OCT compound (Sakura Finetek, Torrance, CA, USA), frozen in liquid nitrogen and stored at −80°C until analysis. Detection of IDO-expressed cells in liver sections was performed using goat polyclonal antibodies directed against rat IDO (I-17; Santa Cruz Biotechnology, Santa Cruz, CA, USA). Cryosections (5 μm thick) were fixed in ice-cold acetone at −20°C for 5 min. After fixation and air drying, the specimens were washed two times with PBS and were blocked by DAKO antibody diluent (DAKO Cytomation, Glostrup, Denmark) for 10 min at room temperature. After the blocking buffer was discarded, sections were incubated at room temperature for 2 h with IDO Ab (1:200 dilution) in blocking buffer, rinsed with five changes of PBS for 5 min and then incubated in Alexa fluorescein-isothiocyanate (FITC)-conjugated donkey antigoat IgG (1:1000 dilution) (Molecular Probe; Invitrogen) for 30 min. The sections were then subjected to a further three 5-min washes in PBS buffer and mounted in Gel/Mount solution (Biomeda, Foster City, CA, USA). To verify which cells would express IDO in the OLT-liver section, we performed double immunostaining. The monoclonal anti-ED1 Ab that detects liver antigen presenting cells (APC) (1:1000 dilution; BMA Biomedicals, Augst, Switzerland) was applied, respectively, and Alexa rhodamine-conjugated donkey antimouse IgG (1:1000 dilution; Molecular Probe; Invitrogen) was used to show another fluorescence signal. All sections were examined using an Olympus BX50 fluorescence microscope (Tokyo, Japan).

Preparation of liver extracts and western blot analysis

To detect the protein level of IDO in liver graft after OLT, naïve DA liver and DA-PVG tolerogeneic OLT liver graft were manually homogenized with T-PER® Tissue Protein Extraction Reagent (PIERCE, Rockford, IL, USA) supplemented with protease inhibitor complete (Roche Diagnostics). After centrifugation, liver extracts were run on a 10% sodium dodecylsulfate–polyacrylamide gel electrophoresis (SDS-PAGE) gel using a mini gel apparatus (BIO-RAD, Burlington, MA, USA), and fractionated proteins were electronically transferred onto a PVDF transfer membrane (GE Healthcare Bio-Sciences). The membrane was blocked using 5% skim milk at room temperature for 1 h and immunoprobed with goat polyclonal antibodies directed against rat IDO (I-17) (1:5000 dilution; Santa Cruz Biotechnology) and peroxidase-conjugated donkey antigoat IgG (1:50 000 dilution; Santa Cruz Biotechnology). Signals were visualized by an Immobilon Western Chemiluminescent HRP substrate (Millipore, Bedford, MA, USA). For internal control, rabbit antiactin (I-19)-R (1:2000 dilution; Santa Cruz Biotechnology) and peroxidase-conjugated goat antirabbit IgG (1:50 000 dilution; Jackson ImmunoResearch Laboratories, West Grove, PA, USA) was used for primary and secondary antibody, respectively.

Statistical analysis

Statistical analysis was performed using Student's *t*-test. A confidence level of $P < 0.05$ was evaluated as significant. Each sample was tested in triplicate, and data were indicated as the mean ± standard deviation (SD).

Results

Suppression of allogeneic mixed lymphocyte reaction by IDO

We tested the immunosuppressive activity of IDO by MLR assay and found that IDO significantly inhibited allogeneic lymphocyte proliferation (Fig. 1). This MLR inhibitory activity of IDO could be significantly abrogated by adding tryptophan (300 μM) or IDO inhibitor (1-MT; 2 nM). These data demonstrate that depletion of tryptophan in the culture medium by IDO may suppress MLR. Kynurenine is the main product of tryptophan through IDO

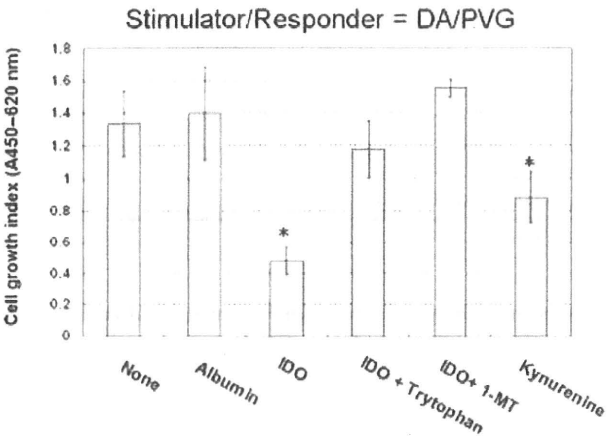

Figure 1 Inhibition of lymphocyte proliferation by indoleamine 2,3-dioxygenase (IDO) in mixed lymphocyte reaction (MLR). IDO (25 μg/mL), tryptophan (300 μM), IDO inhibitor (2 nM) and kynurenine (150 μM) were supplemented into the MLR culture to evaluate their immunological activity. Albumin (25 μg/mL) was used as a control. *Significantly inhibited as compared with positive control (DA-PVG, none) ($P < 0.05$). 1-MT, 1-methyl-DL-tryptophan.

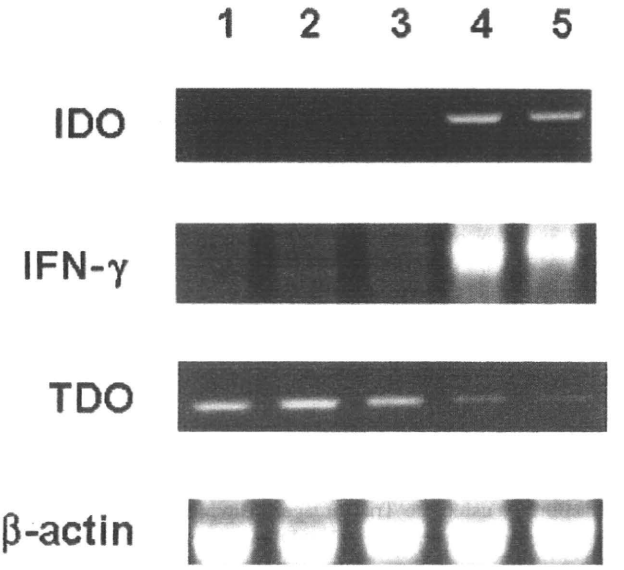

Figure 2 Indoleamine 2,3-dioxygenase (*IDO*) gene expression in rat liver. Reverse transcription–polymerase chain reaction products obtained using primers of IDO, interferon (IFN)-γ, tryptophan 2,3-dioxygenase (TDO) and β-actin were run on a 2% agarose gel. Lane 1, naïve DA liver; lane 2, naïve PVG liver; lane 3, syngeneic orthotopic liver transplantation (OLT) liver (DA to DA, POD 7); lane 4, allogeneic OLT liver (DA to PVG, POD 7); lane 5, allogeneic OLT liver (DA to LEW, POD 7).

catabolism pathway. Recent work has provided definite evidence for an important role of kynurenine metabolites in IDO-mediated modulation of immune function,[40] as well as in IDO-dependent apoptosis of thymocytes and terminally differentiated antigen-specific $CD4^+$ T cells.[41] In our MLR experiment, we also observed the immune suppressive activity of kynurenine (150 μM) (Fig. 1).

Expression of the *IDO* gene in liver allografts

To investigate whether the *IDO* gene is expressed in the liver graft during the acute rejection phase, we collected the day 7 livers from syngeneic OLT (DA-DA) and allogeneic OLT (DA-PVG or DA-LEW) rats. We performed RT-PCR amplifications with rat IDO-specific primers on five samples in duplicate. Histological examination of the DA liver grafts in either PVG or LEW recipients showed severe acute rejection on day 7, with portal and lobular inflammation, biliary epithelial injury and endothelialitis (data not shown). The *IDO* gene expression was upregulated in the allogeneic OLT liver tissue (DA to PVG, DA to LEW) (Fig. 2). However, IDO mRNA expression could not be detected in the naïve (DA or PVG) livers or in the syngeneic OLT (DA-DA) livers. The pattern of gene expression of IFN-γ is similar to that of IDO. TDO mRNA expression in allogeneic livers is lower than that in the naïve and syngeneic livers, suggesting the damage of hepatocytes in the allogeneic OLT livers.

Time-course of *IDO* gene expression in OLT livers (DA-PVG) (spontaneous tolerance model)

In the spontaneous tolerance model, we next investigated the IDO mRNA expression in OLT livers at different phases including the rejection phase postoperative day (POD 7–21), induction phase (POD 21–40) and maintenance phase (POD 40–80) of tolerance OLT (DA-PVG). Histological examination of the DA liver grafts in PVG recipients showed infiltrative leukocytes in both the rejection and induction phases that gradually disappeared during the maintenance phase (data not shown). The IDO mRNA expression was detected in both the rejection and induction phases, and it was gradually downregulated in the maintenance phase (Fig. 3a). β-Actin expression was used as an internal control and relative ratio of *IDO* gene expression to β-actin is shown in Fig. 3b.

Time-course of *IDO* gene expression in OLT livers (DA-LEW + CsA) (drug-induced acceptance model)

Orthotopic liver transplantation (DA-LEW) rats treated with CsA (POD 0–14) can survive for more than 233 days and are designated as a drug-induced acceptance model. Histological examination of the DA liver grafts in LEW recipients showed few infiltrative leukocytes on POD 3–14 and a gradually increasing number of infiltrative leukocytes on POD 70–233 (data not shown). IDO mRNA expression could not be detected in the liver during immunosuppressive treatment (POD 3, 9 and 14), and it was gradually upregulated in the later phase (POD 70, 200 and 233) (Fig. 4a). β-Actin expression was used as an internal control and the relative ratio of *IDO* gene expression to β-actin is shown in Fig. 4b.

Localization of *IDO* gene expression and the effect of CsA on *IDO* gene expression

To investigate localization of the *IDO* gene in the OLT liver during rejection, we focused on the OLT rejection model (DA to LEW, POD 7) and compared the *IDO* gene expression in different organs

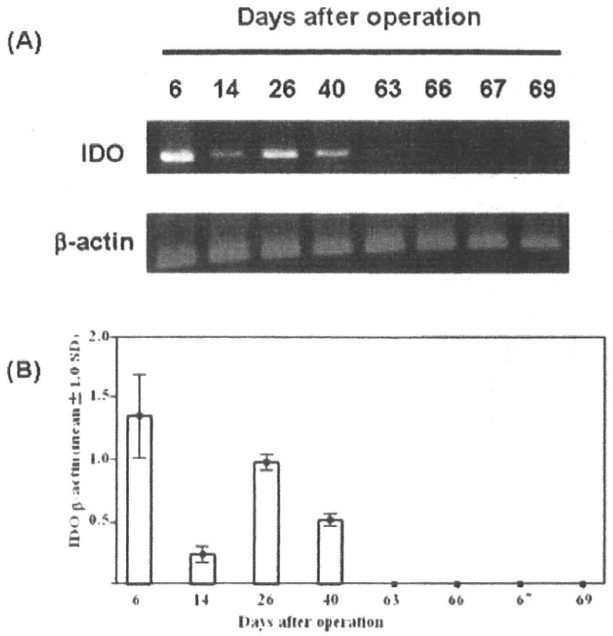

Figure 3 Time-course of indoleamine 2,3-dioxygenase (*IDO*) gene expression in orthotopic liver transplantation (OLT) livers (DA to PVG) (spontaneous tolerance model). (a) Reverse transcription–polymerase chain reaction products obtained using primers of IDO and β-actin were run on a 2% agarose gel. (b) Relative expression of *IDO* gene to β-actin, which was calculated by the TotalLab software. Bars represent the average of density values from two independent experiments.

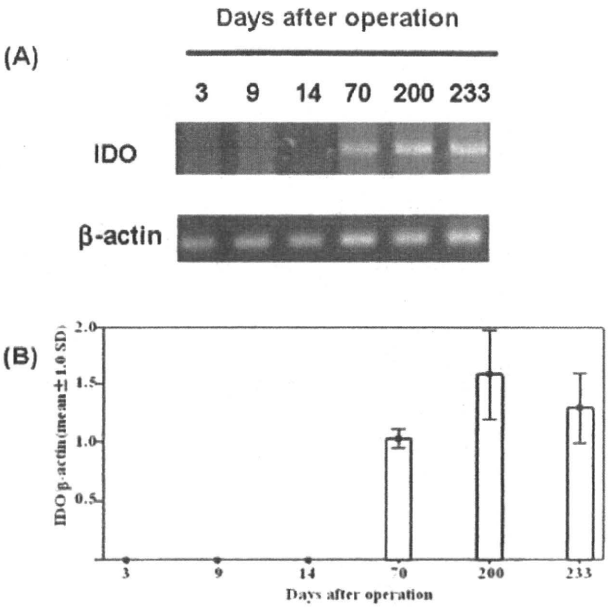

Figure 4 Time-course of indoleamine 2,3-dioxygenase (*IDO*) gene expression in orthotopic liver transplantation (OLT) livers (DA-LEW + cyclosporinee A) (drug-induced acceptance model). (a) Reverse transcription–polymerase chain products obtained using primers of IDO and β-actin were run on a 2% agarose gel. (b) Relative expression of *IDO* gene to β-actin, which was calculated by the TotalLab software. Bars represent the average of density values from two independent experiments.

and cell fractions of the OLT rat liver (Fig. 5). IDO mRNA was detected in the liver, spleen and NPC fraction but not in the PC fraction. However, the CsA-treated OLT model showed no IDO mRNA expression in the liver, spleen, NPC fraction or PC fraction (Fig. 5).

Immunohistochemical and western analyses of IDO in the OLT liver

To investigate which cells express IDO protein in the liver tissue, we performed immunohistochemistry of frozen liver sections which were collected from the tolerance OLT model (DA to PVG, POD 7) and the acute rejection model (DA to LEW, POD 7). The tissue sections were double immunolabeled with antirat IDO (FITC-conjugated, green color) plus anti-ED1 (rhodamine-conjugated, red color). ED1 is useful for the detection of rat APC such as macrophages and dendritic cells,[42] the staining pattern of macrophages identified by ED1 in liver is branched.[43] Under microscopic observation, the IDO-positive cells (green color, Fig. 6A-a) were found in the liver section and these signals were also located on the APC-like cells (red color, Fig. 6A-b). The yellow color cells shown in the merged field are the double-positive cells (Fig. 6A-c). Actually, the immunostain of the two groups showed that the same pattern and IDO protein was located in the APC-like cells. This observation is same as the RNA expression pattern in these two groups. However, we found a higher level of IDO protein which was produced not only in the liver but also

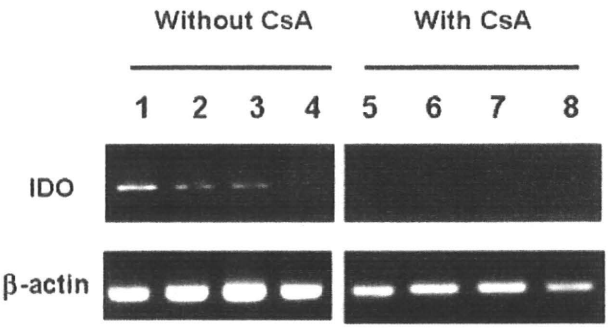

Figure 5 Indoleamine 2,3-dioxygenase (*IDO*) gene expression in the organs and cellular fractions of rejection orthotopic liver transplantation (OLT) rats (DA-LEW, POD 7) without or with cyclosporinee A (CsA) treatment. Lanes 1 and 5, liver of OLT rat; Lanes 2 and 6, spleen of OLT rat; Lanes 3 and 7, non-parenchymal cell fraction of OLT liver; Lanes 4 and 8, parenchymal cell fraction of OLT liver.

in other organs after overcoming rejection (POD 21) and the subsequent tolerance phase after OLT (POD 60, $n = 3$) in a rat tolerance OLT model (DA-PVG) (Fig. 6B).

Discussion

In the present study, we first demonstrated that IDO itself and the tryptophan metabolites (kynurenine) possess immunosuppressive

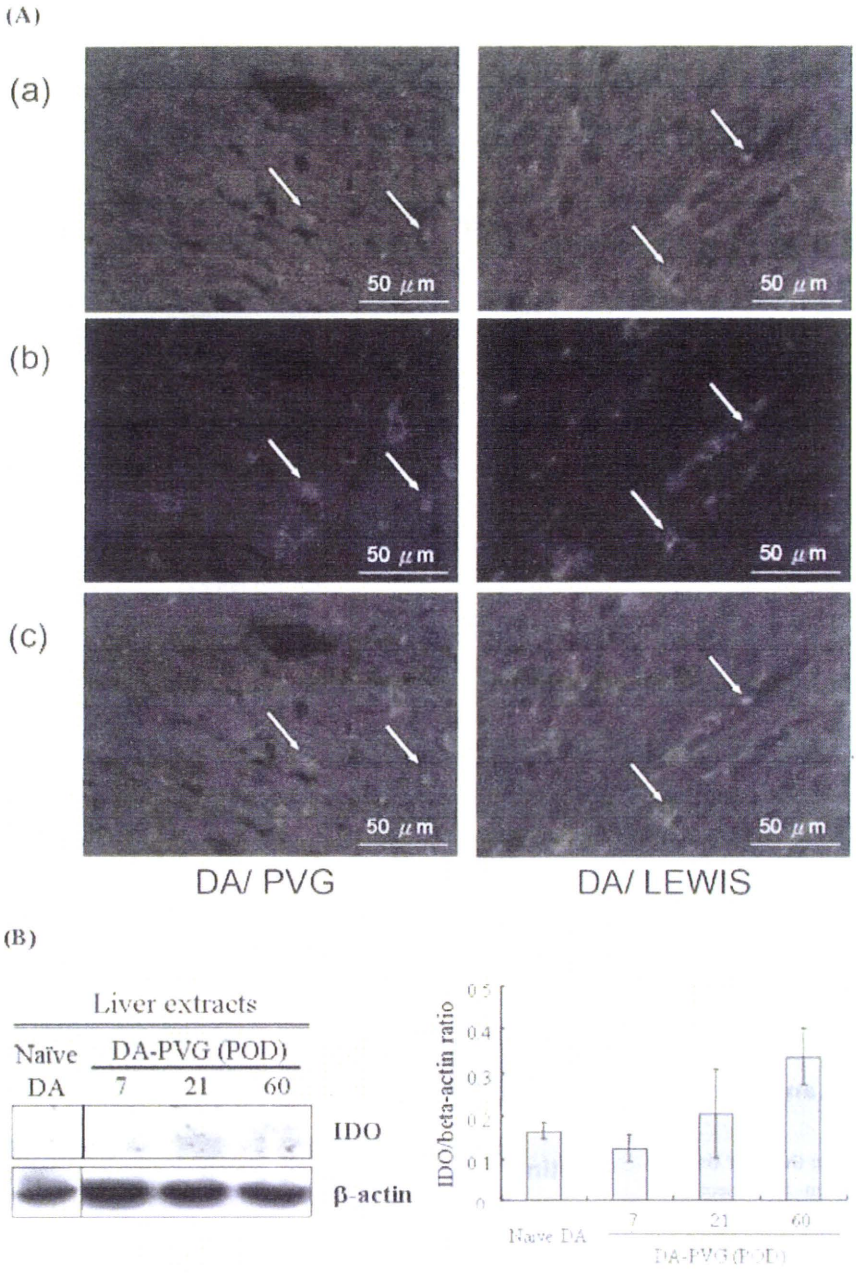

Figure 6 (A) Immunohistochemistry of the liver section in DA-PVG and DA-LEW orthotopic liver transplantation (OLT) rats (POD 7). The frozen sections of OLT liver were doubly stained with antibodies against indoleamine 2,3-dioxygenase (IDO; green) in combination with anti-ED1 (red). The green cells in the field are IDO-positive cells (a). Red cells in the field are antigen-presenting cells such as macrophages or dendritic cells (b). Yellow color cells shown in the merged field are double-positive cells (c). (B) The protein level of IDO in liver extracts of DA-PVG OLT rats. Liver extracts were run on SDS-PAGE and then subjected to western blot analysis. Bars (IDO/β-actin ratio) indicate the average density values from two independent experiments.

activity in MLR. We also revealed *IDO* gene expression in the allogeneic liver grafts (DA liver into PVG rat, DA liver into LEW rat) at the acute rejection phase following OLT. The signal could not be detected when these OLT rats were treated with CsA. Interestingly, IDO expression was detected in both models of tolerance OLT (DA-PVG) and rejection OLT (DA-LEW). Furthermore, time-course study of *IDO* gene expression in the liver grafts of spontaneous tolerance OLT model (DA to PVG) demonstrated that the IDO mRNA is expressed in both the rejection and induction phases, but the signal gradually decreased during the maintenance phase. In contrast, IDO expression gradually appeared in a drug-induced acceptance OLT (DA-LEW + CsA) model after the cessation of CsA. Furthermore, we demonstrated that IDO expression is not seen in hepatocytes but in NPC, such as APC, during rejection.

Recent studies have provided immunosuppressive evidence of tryptophan metabolites (e.g. kynurenine, 3-hydroxykynurenine and 3-hydroxyanthranilic acid) which are the bioactive intermediates of tryptophan catabolism by IDO.[40,44] Another study has demonstrated that T-cell apoptosis was induced by a relatively lower concentration of kynurenine irrespective of Fas–Fas ligand interaction.[41]

In the present study, kynurenine also showed an inhibitory effect on lymphocyte proliferation in MLR. In fact, Miki *et al.*

Journal of Gastroenterology and Hepatology **23** (2008) e243–e250

demonstrated that an IDO inhibitor blocked liver allograft tolerance and induced rejection in a mouse OLT model.[34] However, the molecular basis for this observation has not yet been completely delineated.

We investigated the time-course of mRNA IDO expression in the livers of spontaneous tolerance OLT (DA-PVG), acute rejection OLT (DA-LEW) and drug-induced acceptance OLT (DA-LEW + 2-week CsA) rats. Interestingly, IDO expression was observed during the rejection phase not only in spontaneous tolerance, but also in acute rejection OLT livers; whereas IDO expression was not detected in the acute rejection OLT livers with CsA treatment. These results suggest that IDO expression may reflect the status of natural alloimmunity in the recipients without the immunosuppressive drug. The difference of survival between tolerance OLT (DA-PVG) and rejection OLT (DA-LEW) may depend on the difference of recipients' (PVG or LEW) alloresponse against DA donor livers. We speculate that the immunosuppressive activity of IDO may be strong enough to overcome the acute rejection occurring in tolerance OLT (DA-PVG) by suppressing PVG T-cell proliferation against DA antigens, but it may not be potent enough to suppress LEW T-cell alloimmune response during acute rejection in rejection OLT (DA-LEW) rats. This drug-free tolerance OLT subject may require naturally inducible immunosuppressive proteins to maintain the tolerance state. However, IDO may not be essentially produced in the liver after complete establishment of tolerance. Alternatively, circulating IDO proteins, which are produced by other organ-derived cells and/or immigrating cells in liver grafts, may be accumulated in the liver graft to systematically regulate the host immune system and to maintain tolerance status. As a support to our finding, Laurence *et al.* demonstrated that IDO expression in the spleen was 16-fold greater in tolerance OLT recipients compared to the rejection OLT recipients.[45]

In the present study, we clearly showed that IDO mRNA was expressed in the fraction of NPC but not in that of PC of liver allograft, whereas IDO expression could not be detected in either type of cell fraction from the CsA-treated OLT rats. The NPC fraction contains many APC such as DC or macrophages which are in charge of regulating the immune response to allografts. Although our immunohistochemistry studies using allogeneic OLT livers showed that IDO is expressed in the macrophage-like cells in transplanted livers, these IDO-positive cells may be not only resident macrophages or donor-derived DC but also infiltrating cells, including circulating recipient-derived macrophages or DC. Recently, many reports have indicated that IDO-expressing APC, such as macrophages or DC, inhibit T-cell proliferation via the depletion of tryptophan[26,27] and is responsible for the modulation of mature DC function.[46,47] Further investigation is currently underway to elucidate the functional role of IDO on DC maturation in the rat tolerance OLT model.

Recently, *in vivo* experiments had demonstrated that transplantation of IDO-overexpressing cells or organs was found to significantly extend survival in recipients. For example, IDO expression in transplanted mouse islets prolonged graft survival after adoptive transfer of diabetogenic splenocytes.[30] Engraftment of IDO-expressing xenogeneic fibroblasts populated in a collagen matrix could be immunoprotected in an animal model.[31] IDO overexpression in lung allografts resulted in a significant protective effect with improvement in both functional properties and histological appearance.[32] Overexpression of IDO in donor corneal allografts resulted in prolonged graft survival.[33] We previously observed that the adenovirally IDO-transduced hepatocytes were found to survive longer than vehicle control group in allogeneic hepatocyte transplantation (Lin *et al.*, unpubl. data, 2006). Our and others' findings suggest that IDO may have an application in promoting the engraftment of transplanted cells and/or organs.

In conclusion, we reported herein that the *IDO* gene was detected in the allogeneic liver graft and the IDO-expressing cells were detected in the fraction of NPC but not in that of PC of liver allograft. The immunohistochemistry confirmed that the IDO protein was detected in antigen-presenting cells but not in hepatocytes. These finding suggest that local expression of immunomodulatory molecules on APC-like cells in transplanted organs may regulate the recognition of donor antigen and inhibit further recipient T-cell activation.

Acknowledgments

This work was supported by grants from the Chang Gung Memorial Hospital (CMRPG-83061) and the National Science Council (NSC 94-2314-B-182A-077) of Taiwan.

References

1 Calne RY, Sells RA, Pena JR *et al.* Induction of immunological tolerance by porcine liver allografts. *Nature* 1969; **223**: 472–6.
2 Kamada N, Davies HS, Roser B. Reversal of transplantation immunity by liver grafting. *Nature* 1981; **292**: 840–2.
3 Kamada N, Brons G, Davies HS. Fully allogeneic liver grafting in rats induces a state of systemic nonreactivity to donor transplantation antigens. *Transplantation* 1980; **29**: 429–31.
4 Davies HS, Pollard SG, Calne RY. Soluble HLA antigens in the circulation of liver graft recipients. *Transplantation* 1989; **47**: 524–7.
5 Zavazava N, Kronke M. Soluble HLA class I molecules induce apoptosis in alloreactive cytotoxic T lymphocytes. *Nat. Med.* 1996; **2**: 1005–10.
6 Qian S, Lu L, Fu F *et al.* Apoptosis within spontaneously accepted mouse liver allografts: evidence for deletion of cytotoxic T cells and implications for tolerance induction. *J. Immunol.* 1997; **158**: 4654–61.
7 Bertolino P, Trescol-Biemont MC, Thomas J *et al.* Death by neglect as a deletional mechanism of peripheral tolerance. *Int. Immunol.* 1999; **11**: 1225–38.
8 Celli S, Matzinger P. Liver transplants induce deletion of liver-specific T cells. *Transplant. Proc.* 2001; **33**: 102–3.
9 Kamada N. The immunology of experimental liver transplantation in the rat. *Immunology* 1985; **55**: 369–89.
10 Kobayashi E, Kamada N, Enosawa S *et al.* Prevention by liver transplantation of the graft-versus-host reaction and allograft rejection in a rat model of small bowel transplantation. *Transplantation* 1994; **57**: 177–81.
11 Tsurufuji M, Ishiguro K, Shinomiya T, Uchida T, Kamada N. Immunosuppressive activity of serum from liver-grafted rats: in vitro specific inhibition of mixed lymphocyte reactivity by antibodies against class II RT1 alloantigens. *Immunology* 1987; **61**: 421–8.
12 Sun J, Sheil AG, Wang C *et al.* Tolerance to rat liver allografts: IV. Acceptance depends on the quantity of donor tissue and on donor leukocytes. *Transplantation* 1996; **62**: 1725–30.
13 Otto C, Kauczok J, Martens N *et al.* Mechanisms of tolerance induction after rat liver transplantation: intrahepatic CD4(+) T cells

produce different cytokines during rejection and tolerance in response to stimulation. *J. Gastrointest. Surg.* 2002; **6**: 455–63.
14 Sun Z, Wada T, Maemura K *et al.* Hepatic allograft-derived Kupffer cells regulate T cell response in rats. *Liver Transpl.* 2003; **9**: 489–97.
15 Olver S, Goto S, Chiba S, Clouston A, Kelso A. Persistence of donor-reactive CD4+ T cells in liver and spleen of rats tolerant to a liver allograft. *Transplantation* 1998; **66**: 132–5.
16 Starzl TE, Murase N, Thomson A, Demetris AJ. Liver transplants contribute to their own success. *Nat. Med.* 1996; **2**: 163–5.
17 Ricordi C, Karatzas T, Nery J *et al.* High-dose donor bone marrow infusions to enhance allograft survival: the effect of timing. *Transplantation* 1997; **63**: 7–11.
18 Thomson AW, Lu L, Murase N *et al.* Microchimerism, dendritic cell progenitors and transplantation tolerance. *Stem Cells* 1995; **13**: 622–39.
19 Starzl TE, Demetris AJ, Murase N *et al.* Cell migration, chimerism, and graft acceptance. *Lancet* 1992; **339**: 1579–82.
20 Lord R, Vari F, Goto S, Sunagawa M. Antigen presenting cells and chimerism. *Transpl. Immunol.* 1998; **6**: 61–3.
21 Kamada N, Goto S, Lord R, Kobayashi E, Kim YI. Novel immunosuppressive proteins induced in rats by liver retransplantation. *Transplant. Proc.* 1995; **27**: 402–3.
22 Bishop GA, Sun J, DeCruz DJ *et al.* Tolerance to rat liver allografts. III. Donor cell migration and tolerance-associated cytokine production in peripheral lymphoid tissues. *J. Immunol.* 1996; **156**: 4925–31.
23 Kobayashi S, Lord R, Goto S *et al.* Production of IL-2 by hepatocytes in allografted liver of rats. *Transpl. Immunol.* 1997; **5**: 237–9.
24 Moffett-King A. Natural killer cells and pregnancy. *Nat. Rev. Immunol.* 2002; **2**: 656–63.
25 Munn DH, Zhou M, Attwood JT *et al.* Prevention of allogeneic fetal rejection by tryptophan catabolism. *Science* 1998; **281**: 1191–3.
26 Munn DH, Shafizadeh E, Attwood JT *et al.* Inhibition of T cell proliferation by macrophage tryptophan catabolism. *J. Exp. Med.* 1999; **189**: 1363–72.
27 Hwu P, Du MX, Lapointe R *et al.* Indoleamine 2,3-dioxygenase production by human dendritic cells results in the inhibition of T cell proliferation. *J. Immunol.* 2000; **164**: 3596–9.
28 Kai S, Goto S, Tahara K *et al.* Inhibition of indoleamine 2,3-dioxygenase suppresses NK cell activity and accelerates tumor growth. *J. Exp. Ther. Oncol.* 2003; **3**: 336–45.
29 Kai S, Goto S, Tahara K *et al.* Indoleamine 2,3-dioxygenase is necessary for cytolytic activity of natural killer cells. *Scand. J. Immunol.* 2004; **59**: 177–82.
30 Alexander AM, Crawford M, Bertera S *et al.* Indoleamine 2,3-dioxygenase expression in transplanted NOD islets prolongs graft survival after adoptive transfer of diabetogenic splenocytes. *Diabetes* 2002; **51**: 356–65.
31 Li Y, Tredget EE, Ghaffari A *et al.* Local expression of indoleamine 2,3-dioxygenase protects engraftment of xenogeneic skin substitute. *J. Invest. Dermatol.* 2006; **126**: 128–36.
32 Liu H, Liu L, Fletcher BS, Visner GA. Novel action of indoleamine 2,3-dioxygenase attenuating acute lung allograft injury. *Am. J. Respir. Crit. Care Med.* 2006; **173**: 566–72.
33 Beutelspacher SC, Pillai R, Watson MP *et al.* Function of indoleamine 2,3-dioxygenase in corneal allograft rejection and prolongation of allograft survival by over-expression. *Eur. J. Immunol.* 2006; **36**: 690–700.
34 Miki T, Sun H, Lee Y *et al.* Blockade of tryptophan catabolism prevents spontaneous tolerogenicity of liver allografts. *Transplant. Proc.* 2001; **33**: 129–30.
35 Pan TL, Lin CL, Chen CL *et al.* Identification of the indoleamine 2,3-dioxygenase nucleotide sequence in a rat liver transplant model. *Transpl. Immunol.* 2000; **8**: 189–94.
36 Nakano T, Kawamoto S, Lai CY *et al.* Liver transplantation-induced antihistone H1 autoantibodies suppress mixed lymphocyte reaction. *Transplantation* 2004; **77**: 1595–603.
37 Kamada N, Calne RY. A surgical experience with five hundred thirty liver transplants in the rat. *Surgery* 1983; **93**: 64–9.
38 Lord R, Goto S, Vari F *et al.* Differences in the rate of donor leucocyte migration between natural and drug-assisted tolerance following rat liver transplantation. *Clin. Exp. Immunol.* 1997; **108**: 358–65.
39 Tateno C, Takai-Kajihara K, Yamasaki C, Sato H, Yoshizato K. Heterogeneity of growth potential of adult rat hepatocytes in vitro. *Hepatology* 2000; **31**: 65–74.
40 Temess P, Bauer TM, Rose L *et al.* Inhibition of allogeneic T cell proliferation by indoleamine 2,3-dioxygenase-expressing dendritic cells: mediation of suppression by tryptophan metabolites. *J. Exp. Med.* 2002; **196**: 447–57.
41 Fallarino F, Grohmann U, Vacca C *et al.* T cell apoptosis by kynurenines. *Adv. Exp. Med. Biol.* 2003; **527**: 183–90.
42 Damoiseaux JG, Dopp EA, Calame W *et al.* Rat macrophage lysosomal membrane antigen recognized by monoclonal antibody ED1. *Immunology* 1994; **83**: 140–7.
43 Dijkstra CD, Dopp EA, Joling P, Kraal G. The heterogeneity of mononuclear phagocytes in lymphoid organs: distinct macrophage subpopulations in the rat recognized by monoclonal antibodies ED1, ED2 and ED3. *Immunology* 1985; **54**: 589–99.
44 Bauer TM, Jiga LP, Chuang JJ *et al.* Studying the immunosuppressive role of indoleamine 2,3-dioxygenase: tryptophan metabolites suppress rat allogeneic T-cell responses in vitro and in vivo. *Transpl. Int.* 2005; **18**: 95–100.
45 Laurence JM, Wang C, Park T *et al.* The role of tryptophan metabolism in rat liver transplant tolerance. *Transplantation* 2006; **82**: 889.
46 Munn DH, Sharma MD, Lee JR *et al.* Potential regulatory function of human dendritic cells expressing indoleamine 2,3-dioxygenase. *Science* 2002; **297**: 1867–70.
47 Grohmann U, Fallarino F, Puccetti P. Tolerance, DCs and tryptophan: much ado about IDO. *Trends Immunol.* 2003; **24**: 242–8.